

A high-resolution diatom record of late-Quaternary sea-surface temperatures and oceanographic conditions from the eastern Norwegian Sea

CHRISTOPHER J. A. BIRKS AND NALÂN KOÇ

BOREAS



Birks, C. J. A. & Koç, N. 2002 (December): A high-resolution diatom record of late-Quaternary sea-surface temperatures and oceanographic conditions from the eastern Norwegian Sea. *Boreas*, Vol. 31, pp. 323–344. Oslo. ISSN 0300-9483.

Core MD95-2011 was taken from the eastern Vøring Plateau, near the Norwegian coast. The section between 250 and 750 cm covers the time period from 13 000 to 2700 cal. yr BP (the Lateglacial and much of the Holocene). Samples at 5 cm intervals were analysed for fossil diatoms. A data-set of 139 modern sea-surface diatom samples was related to contemporary sea-surface temperatures (SSTs) using two different numerical methods. The resulting transfer functions were used to reconstruct past sea-surface temperatures from the fossil diatom assemblages. After the cold Younger Dryas with summer SSTs about 6°C, temperatures warmed rapidly to about 13°C. One of the fluctuations in the earliest Holocene can be related to the Pre-Boreal Oscillation, but SSTs were generally unstable until about 9700 cal. yr BP. Evidence from diatom concentration and magnetic susceptibility suggests a change and stabilization of water currents associated with the final melting of the Scandinavian Ice Sheet at c. 8100 cal. yr BP. A period of maximum warmth between 9700 and 6700 cal. yr BP had SSTs 3–5°C warmer than at present. Temperatures cooled gradually until c. 3000 cal. yr BP, and then rose slightly around 2750 cal. yr BP. The varimax factors derived from the Imbrie & Kipp method for sea-surface-temperature reconstructions can be interpreted as water-masses. They show a dominance of Arctic Waters and Sea Ice during the Younger Dryas. The North Atlantic current increased rapidly in strength during the early Holocene, resulting in warmer conditions than previously. Since about 7250 cal. yr BP, Norwegian Atlantic Water gradually replaced the North Atlantic Water, and this, in combination with decreasing summer insolation, led to a gradual cooling of the sea surface. Terrestrial systems in Norway and Iceland responded to this cooling and the increased supply of moisture by renewed glaciation. Periods of glacial advance can be correlated with cool oscillations in the SST reconstructions. By comparison with records of SSTs from other sites in the Norwegian Sea, spatial and temporal changes in patterns of ocean water-masses are reconstructed, to reveal a complex system of feedbacks and influences on the climate of the North Atlantic and Norway.

Christopher J. A. Birks (e-mail: chris.birks@bot.uib.no), Department of Geology, University of Bergen, Allégaten 41, NO-5007 Bergen, Norway (address for correspondence: Botanical Institute, University of Bergen, Allégaten 41, NO-5007 Bergen, Norway); Nalân Koç (e-mail: nalan.koc@npolar.no), Norwegian Polar Institute, NO-9296 Tromsø, Norway; received 2nd July 2001, accepted 21st March 2002.

The Nordic Seas are a critical area of oceanographic dynamics, both locally and globally. During the last glacial termination and the Holocene, the Nordic Seas experienced considerable climatic and oceanographic changes, summarized by the maps of Koç *et al.* (1993) and Koç & Jansen (1994). Using data from the core sites shown in Fig. 1, Koç *et al.* (1993) reconstructed the penetration of Atlantic Waters during the Younger Dryas (12 700–11 550 cal. yr BP) which formed an early ice-free area along the Norwegian coast and they mapped the movements of the Polar and Arctic fronts northwestwards during the early Holocene and the development of the Holocene oceanic circulation pattern. The Vøring Plateau (Fig. 1) is in a sensitive position regarding these developments as it should lie under the proposed Lateglacial ice-free passage and it should be affected in the first stages of the entry and development of North Atlantic Waters in the Holocene. New data from there are needed to test and strengthen these reconstructions.

Therefore, to help fill gaps in the spatial data of Koç *et al.* (1993) and thus to position more precisely the

boundary areas and progress of ice-melting and ocean current development in space and time, core MD95-2011 was selected for study. Its sediments were investigated by diatom analyses at high temporal resolution combined with a radiocarbon chronology and physical measurements on the sediments.

Diatoms respond sensitively and rapidly to environmental changes (e.g. Sancetta 1999), expanding and contracting their populations and ranges as environmental factors change over time. Assuming that assemblages in surface-sediments represent the composition of the contemporary diatom populations living in the photic zone, the composition of modern diatom surface-sediment assemblages can be related quantitatively by an empirically derived transfer function to contemporary sea-surface conditions, such as temperatures. Using such a transfer function, fossil assemblages in a sediment core can be used to make quantitative reconstructions of past sea-surface temperatures (SSTs) for the time span represented by the sediment record.

This study uses diatom analysis to reconstruct past SSTs and related palaeoceanographic conditions at the

Vøring Plateau at a much higher temporal resolution for the early and mid-Holocene than was previously available from the eastern Norwegian Sea. The results are compared with previous studies (Fig. 1) in order to reconstruct temporal and spatial patterns in SSTs and variations in palaeoceanographic conditions through the Younger Dryas and most of the Holocene. An enlarged modern data-set of surface samples covering a wider SST range than that available to Koç *et al.* (1993) has been used in this study, and it has also been applied for direct comparison to the most detailed currently available Lateglacial and Holocene data, HM79-6/4, situated south of MD95-2011 (Fig. 1).

Study site

The North Atlantic current conveys large quantities of heat to northern latitudes, and variations in its flow also influence the climate of the land. With modern summer SSTs of 11–6°C and winter SSTs between 8°C and 3°C, it flows parallel to the Norwegian coastal current along Norway until it meets cold Polar Water with SSTs between –1.5°C and 0°C and forms the Barents Sea

Polar Front (Hopkins 1991; Lozier *et al.* 1995) (Fig. 1). The cold East Greenland current flows southwards along eastern Greenland and through the Denmark Strait between Greenland and Iceland. Where the two major water-masses meet, they form large circular gyre currents, which are important areas for North Atlantic Deep Water formation that drives the thermohaline circulation (e.g. Damuth 1978). Along the contact line from Iceland to Spitsbergen, two fronts form in the surface waters. To the west, the Polar Front represents the mixing contact between the Polar and Arctic Water-masses (Sarnthein *et al.* 1992). To the east, the Arctic Front represents the mixing contact between the Arctic and Atlantic Water-masses (Johannessen 1986). During winter, the fronts migrate to the east, with a resulting fall in SST, an increased presence of sea ice and colder air temperatures. A major oceanographic feature of the Nordic Seas is sea-ice cover (Fig. 1). The presence of sea ice influences several important physical processes: (1) sea-atmosphere exchange of heat and water, (2) the movement of surface water, (3) brine formation during freezing, and (4) reflection of solar radiation by the strong albedo (Hopkins 1991). Disturbances to the system, e.g. an increase in sea-ice cover, may change

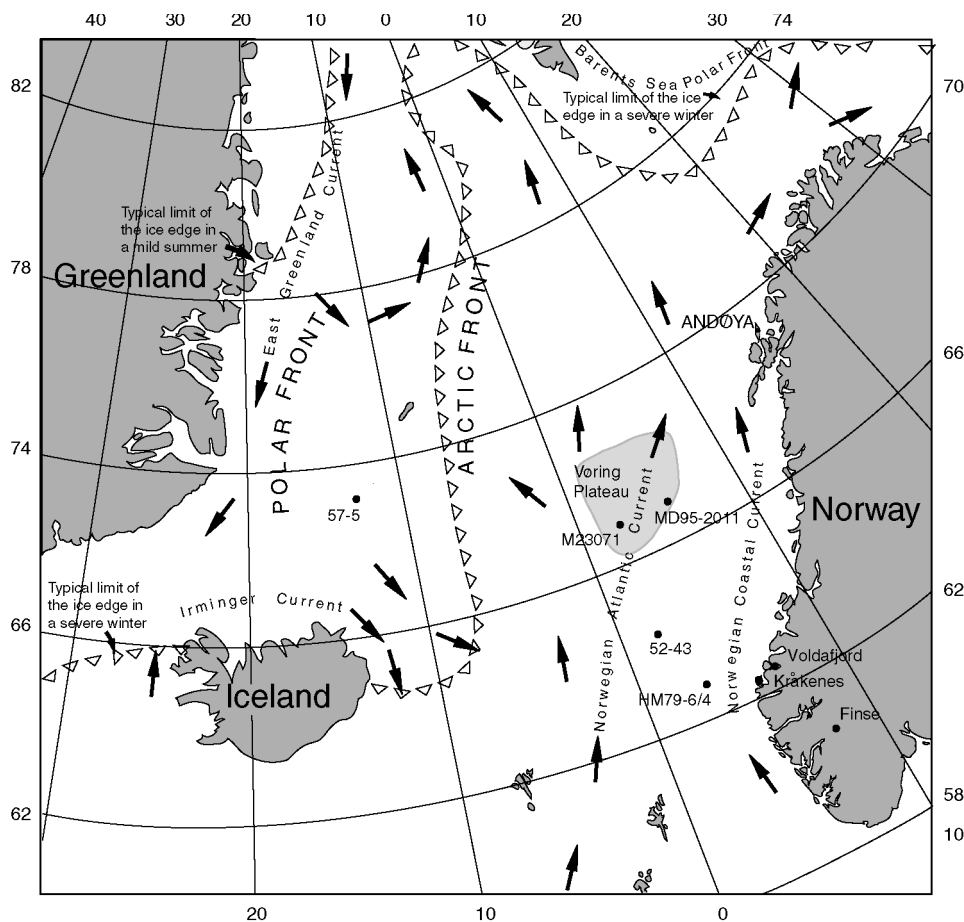


Fig. 1. The Nordic Seas showing the location of the core MD95-2011 on the east side of the Vøring Plateau. Other sites discussed in the text, the main currents, the Polar and Arctic Fronts, and the summer and winter ice-limits are also shown.

the rate of water circulation and exchange, or even stop it altogether (Broecker 1991). With a varying strength of thermohaline turn-around, the sensible heat transport to northern latitudes will change, and climatic conditions in northern Europe and the North Atlantic region will thus be affected (Bradley 1999).

Methods

Coring, subsampling and geophysics

Core MD95-2011 was collected with a Calypso corer from a water depth of 1048 m from *R/V Marion Dufresne* during the IMAGES 101 cruise on 6 August 1995. Its location is 66°58.18'N, 07°38.35'E, on the eastern Vøring Plateau (Fig. 1). The core is 1749 cm long. In this study, the section from 200 cm to 750 cm (Holocene and Younger Dryas) was examined at a sampling interval of 5 cm.

The core was logged and a GEOTEK Ltd Multi Sensor Core Logger or MST (Multi Sensor Track) was used to record three physical properties (Fig. 4): P-wave velocity in the sediment, bulk density and magnetic susceptibility (IMAGES 101 1995). In addition, wet-bulk density, dry-weight density and porosity were measured before the core was subsampled onboard ship.

Diatom analysis

Diatom-sample preparation followed Koç Karpuz (1989) and Koç Karpuz & Schrader (1990). Diatoms were counted using a Leitz Orthoplan microscope (100/1.32 objective). Following Schrader & Gersonde (1978), random transects were examined, and a total of at least 300 valves (excluding *Chaetoceros*) were identified and counted per sample. *Chaetoceros* valves were not used in the percentage calculations or SST reconstructions because (a) they are often so numerous that they can totally dominate the assemblage, thus biasing the reconstructions, and (b) they show little or no sensitivity to SST changes (Koç Karpuz & Schrader 1990). However, *Chaetoceros* valves were counted and used as an indicator of primary productivity.

Diatom concentrations (g^{-1} dry weight of sediment) were estimated following Koç Karpuz (1989) and Schrader *et al.* (1993). Concentration was used as a surrogate for the flux of diatom valves from the photic zone to the sediment and was used as a reflection of primary production (Schrader *et al.* 1993). High diatom concentrations indicate high levels of primary production and/or better preservation rates of valves in the sediment (Koç Karpuz & Jansen 1992). Primary production can be limited by total ice-cover, as diatoms are dependent upon light, but diatoms can be especially abundant at or near ice margins (Williams 1993; Sakshaug & Skjoldal 1989; Sakshaug & Slagstad 1990).

The diatom counts were entered and percentages

calculated and plotted using TILIA and TILIA-GRAPH (Grimm 1990/1) (Fig. 2). The stratigraphical data were divided into assemblage zones using the program ZONE (S. Juggins unpubl.), based on a numerically optimal sum-of-squares partitioning with stratigraphical constraints (Birks & Gordon 1985). The resulting zonation was compared with the 'broken-stick' model (Bennett 1996), and six statistically significant zones were established using the program BSTICK (J. M. Line & H. J. B. Birks unpubl.). The zones are delimited solely on the basis of the data and on stated mathematical criteria, without any reference to inferred climatic conditions or chronology. They are unbiased and can be used as aids in interpretation and discussion.

Diatom nomenclature and taxonomic authorities are given in Appendix 1.

Radiocarbon dating and age-depth modelling

The 5 AMS radiocarbon dates obtained from the 200–750 cm section of core MD95-2011 are listed in Table 1, together with a date at 170.5 cm. They were measured on monospecific samples of *c.* 1500 *Neoglobigerina pachyderma* tests, from the size range 150–250 μm , corresponding to 7–15 mg of carbonate. The ^{14}C date at 510–511 cm was deemed contaminated because of its unexpectedly great age (14540 ± 120 ^{14}C yr BP) and was rejected. The ^{14}C dates were corrected for a marine reservoir age of 400 years (Stuiver *et al.* 1986). Hafliðason *et al.* (2000) used tephrochronology to show that a 400-year reservoir age is reasonable for present and Holocene dates, but during the Younger Dryas and earliest Holocene the reservoir ages were greater by several hundred years. However, none of the dated levels falls within this period, so all were corrected by 400 years. The ^{14}C dates were calibrated using the INTCAL93 data-set and method A in CALIB v3.0.3c (Stuiver & Reimer 1993) in order to achieve consistency and comparability with previous calibrations by Andersen (1998) and Dreger (1999) for core MD95-2011. However, calibrations based on the INTCAL98 data-set and CALIB v4.2 (Stuiver *et al.* 1998) and INTCAL93 are very similar in this age range (Table 1). With only 5 usable ^{14}C dates with long time-intervals between them, simple linear interpolation was considered the most appropriate means of deriving an age-depth model. The date above the core section at 170.5 cm was used to constrain the upper part of the age-depth model. The level interpreted in the SST reconstructions as the onset of the Holocene (695 cm) was assumed to be 11550 cal. yr BP (Gulliksen *et al.* 1998) and this was used to constrain the lower part of the model. The calibrated ages of each sample were estimated from the age-depth model.

Sea-surface temperature reconstructions

A modern calibration data-set of 139 surface samples

Table 1. Radiocarbon dates, corrected ages, and calibrated dates from MD95-2011. Sample GifA 96671 was deemed contaminated and unreliable and was not calibrated or used in the age-depth model.

| Lab number | Mean depth (cm) | Species | ¹⁴ C Age yr BP | Corrected age ¹⁴ C yr BP (–400 yr) | INTCAL93 Calibrated age yr BP (1 std dev.) | INTCAL98 Calibrated age yr BP (1 std dev.) |
|------------|-----------------|--------------------------|---------------------------|---|--|--|
| GifA 96472 | 170.5 | <i>N. pachyderma</i> (d) | 2620 ± 60 | 2220 ± 60 | 2138–2327 | 2132–2334 |
| KIA 10011 | 269.5 | <i>N. pachyderma</i> (d) | 3820 ± 35 | 3420 ± 30 | 3628–3692 | 3635–3693 |
| KIA 463 | 320.5 | <i>N. pachyderma</i> (d) | 4330 ± 50 | 3930 ± 50 | 4286–4418 | 4295–4421 |
| GifA 96671 | 510.5 | <i>N. pachyderma</i> (d) | 14940 ± 120 | 14 540 ± 120 | — | — |
| KIA 464 | 520.5 | <i>N. pachyderma</i> (d) | 7260 ± 60 | 6860 ± 60 | 7582–7683 | 7620–7743 |
| KIA 465 | 750.5 | <i>N. pachyderma</i> (s) | 12 220 ± 90 | 11 820 ± 90 | 13 637–13 932 | 13 615–14 034 |

Table 2. Calibrated ages of the diatom zone boundaries on Fig. 2, rounded to the nearest 5 years.

| Zone | Depth (cm) | Age (cal yr BP) |
|--------|-------------|-----------------|
| Zone 6 | 320–200 | 4400–2665 |
| Zone 5 | 452.5–320 | 6550–4400 |
| Zone 4 | 592.5–452.5 | 9240–6550 |
| Zone 3 | 692.5–592.5 | 11 435–9240 |
| Zone 2 | 742.5–692.5 | 13 450–11 435 |
| Zone 1 | 750–742.5 | 13 765–13 450 |

and August (summer) and February (winter) SSTs (N. Koç unpubl. and Appendix 2) was used to reconstruct palaeotemperatures in MD95-2011. This data-set is enlarged from the calibration data-set used by Koç Karpuz & Schrader (1990), Koç Karpuz & Jansen (1992), Koç *et al.* (1993) and partly by Koç *et al.* (1996). A new SST reconstruction using the Imbrie & Kipp (1971) method was also made for core HM79-6/4 (Koç & Jansen 1992) using the enlarged modern data-set, in order to achieve comparability with the results using both calibration data-sets, and to allow direct comparison of reconstructed temperatures from MD95-2011 and HM79-6/4. This new reconstruction is termed HM79-6/4 v2, whereas the original reconstruction of Koç Karpuz & Jansen (1992) is termed HM79-6/4 v1 (see Fig. 6).

Two palaeoenvironmental reconstruction methods and resulting transfer functions have been applied to core MD95-2011; Imbrie & Kipp's (1971) 'factor analysis regression' (referred to here as I&K) and weighted-averaging partial least squares (WA-PLS) (ter Braak & Juggins 1993). These two methods were selected because (1) the I&K approach is widely used in marine palaeoceanography and (2) WA-PLS, originally developed in palaeolimnology, appears in a range of comparative studies (ter Braak 1995; ter Braak *et al.* 1993; Birks 1995, 1998 and unpubl.) to perform as well or better, as assessed by a range of performance statistics, than other reconstruction procedures. Like the I&K approach, WA-PLS is an 'inverse' regression approach that uses several components in the final transfer function. Unlike the I&K method, WA-PLS assumes unimodal responses of species to their en-

vironment (ter Braak & Juggins 1993). The components are selected in WA-PLS to maximize the covariance between the environmental variable to be reconstructed (e.g. summer SST) and hence to maximize the predictive power of the model. This contrasts with the I&K approach, where the components are chosen irrespective of their predictive value to capture only the maximum variance within the modern biological data. Unlike the I&K method as currently implemented in the programs CABFAC, THREAD and REGRESS written by J. Imbrie and J. E. Klovon and modified by T. Schrader, where the number of components or factors to include is chosen by the user, the number of components included in WA-PLS is based on a statistical leave-one-out cross-validation procedure (ter Braak & Juggins 1993). In leave-one-out cross-validation the inference or 'reconstruction' procedure is applied n times using the modern data-set of size $(n - 1)$. In each of the n inferences, one modern sample is left out in turn and the transfer function based upon the $(n - 1)$ samples in the modern data-set is applied to the one excluded sample to give a predicted value (\hat{x}_i) for the environmental value of that modern sample i . By subtracting the predicted (\hat{x}_i) from the observed value (x_i) a prediction error for the sample can be estimated. These prediction errors are accumulated for all n modern samples to give a root mean square error of prediction (RMSEP), r^2 (the coefficient of determination between observed and predicted values) and maximum bias (ter Braak & Juggins 1993) based on cross-validation (Birks 1995). Statistics based on comparing inferred and observed values in the modern data-set without any cross-validation are called 'apparent' statistics (Birks 1995). The root mean square error (RMSE) is invariably underestimated and r^2 and maximum bias are overestimated when based solely on the modern data-set (Birks 1995; ter Braak & Juggins, 1993). Further details of WA-PLS are given by ter Braak & Juggins (1993), ter Braak (1995), ter Braak *et al.* (1993) and Birks (1995, 1998). WA-PLS was implemented by the program CALIBRATE written by S. Juggins and C. J. F. ter Braak. The program RMSEP written by J. M. Line and H. J. B. Birks was used to calculate bias and other performance statistics for the I&K models.

If a transfer function is to be reliable, it should have a

low RMSEP and maximum bias, and a high correlation (r) or coefficient of determination (r^2) between observed and predicted values (Birks 1995, 1998). Using the combination of low RMSEP and maximum bias, along with a high r^2 (as assessed by leave-one-out cross-validation) and a small number of 'useful' components (Birks 1998), four-component WA-PLS models were selected for both August and February temperatures. An eight-component I&K model was used, following Andersen (1998) and Koç (unpubl.) (see Appendix 2). Both transfer functions used in this study have low RMSE or RMSEP (*c.* 1°C), a high r^2 (*c.* 0.9°C) and a maximum bias of *c.* 1°C. In theory, they are both reliable and robust, at least when evaluated by these statistical criteria based on the modern data only. Their reliability and robustness should, however, be evaluated by their performance when applied to core stratigraphical data. Each method and associated transfer function produces overall similar SST reconstructions but which differ in detail (Fig. 3).

As a by-product of the SST reconstructions produced by the I&K method, the eight varimax 'factors' used in the reconstruction of MD95-2011 are plotted stratigraphically (Fig. 5). Each factor can be interpreted as representing a particular dominant diatom assemblage that may reflect a certain contemporary water-mass (Andersen 1998; Koç Karpuz & Jansen 1992; Koç

Karpuz & Schrader 1990). The eight factors, dominant diatom taxa and inferred water-masses are summarized in Appendix 3. By plotting the factor scores for MD95-2011 on a depth and age basis (Fig. 5), it is possible to see which of the factors and their inferred water-masses may have been dominant throughout the time represented by the core.

Results

Radiocarbon dates and age-depth model

The five AMS ^{14}C dates between 200–750 cm of MD95-2011 and the date at 170.5 cm are shown in Table 1, together with the 400 yr marine reservoir correction and the calibrated ages using INTCAL93 and INTCAL98. The estimated ages of each sample derived from the age-depth model are plotted on the stratigraphical diagrams (Figs 2–5, 7). Before discussing the stratigraphical data, it is necessary to test the reliability and robustness of the age-depth model based on linear interpolation by using stratigraphical markers not used to construct the age-depth model.

The mid-Younger Dryas Vedde Ash was identified in the core over a 45 cm interval by Dreger (1999). Because large amounts of tephra can be transported

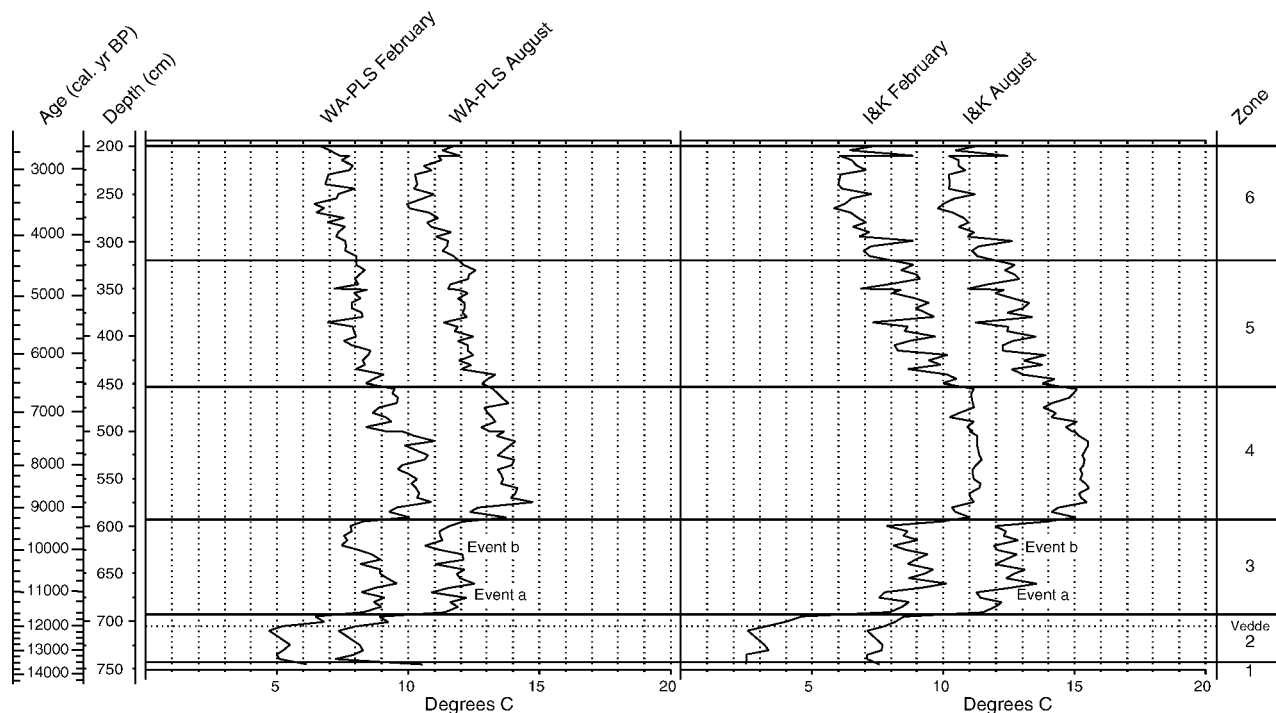


Fig. 3. August and February sea-surface temperature reconstructions (°C) for core MD95-2011 based on Weighted Averaging Partial Least Squares (WA-PLS) and Imbrie & Kipp (1971) (I&K), plotted against depth and estimated age in calibrated years BP. The diatom assemblage zones are also shown. Events a and b are indicated.

by pack ice and bottom currents (e.g. Hafflidason *et al.* 2000), resulting in delayed or extended deposition (e.g. an 800 yr delay in the Iceland Shelf region (Eiríksson *et al.* 2000)), it is not always easy to use the occurrence of ash as an unambiguous time-marker horizon (cf. Lowe & Turney 1997). Therefore, the Vedde Ash was not used in the construction of the age-depth model. The stratigraphic position of its primary occurrence was determined as 700–705 cm by T. Dokken (pers. comm. 2001) (cf. Dreger 1999). The estimated age of this level from the age-depth model is 11 900–12 000 cal. yr BP. This corresponds very closely to the GRIP ice-core age of the Vedde Ash of $11\,980 \pm 80$ ice-core yr BP (Grønvold *et al.* 1995) and the calibrated age of a terrestrial Vedde Ash horizon (c. 12 000 cal. yr BP) (Birks *et al.* 1996, 2000) and suggests that the MD95-2011 age model is reliable in this age range. As a second test of the model, the age of the level interpreted as equivalent to the '8.2 ka event' (Klitgaard-Kristiansen *et al.* 1998), 540 cm, was estimated from the age-depth model to be 8100 cal. BP. The correspondence of these two horizons to expected ages lends credulity to the age-depth model for MD95-2011.

Diatom stratigraphy (Fig. 2), sea-surface temperature reconstructions (Fig. 3) and water-mass reconstructions (Fig. 5)

Zone 1 (750–742.5 cm, 13 765–13 450 cal. yr BP). – Zone 1 (Fig. 2) has a low diatom concentration with no dominant species, and thus does not clearly suggest any dominating factor-inferred water-mass. Of the two samples, that at 750 cm is devoid of diatoms. All the trends (Fig. 3) result from the joined SST curves from zone 1 to zone 2. Both reconstruction methods show cooling to 7–8°C for August (Fig. 3) but the magnitude is only greater than 1°C in the WA-PLS reconstruction. February temperatures reconstructed by I&K are stable. WA-PLS shows a cooling from 6 to 5°C.

Zone 2 (742.5–692.5 cm, 13 450–11 435 cal. yr BP). – Of the 10 samples in zone 2, 2 (720 cm and 715 cm; 12 970–12 835 cal. yr BP) are devoid of diatoms. The base of the Vedde Ash is at 700–705 cm (T. Dokken, pers. comm. 2001). Zone 2 is dominated by high percentages of *Thalassiosira gravida* spores (Fig. 2). This suggests that much of the winter season was influenced by proximal or direct ice-cover (Williams 1986). Zone 2 is also characterized by the presence of arctic-ice species such as *Fragilariopsis oceanica* (Williams 1986), *Bacterosira fragilis* and *Porosira glacialis* (Fig. 2). *P. glacialis* is characteristic of conditions of long-term, fast ice-cover (Williams 1986). These diatoms have few occurrences through the rest of the core. Factor 6, the Arctic Waters and the Polar Front assemblage, dominates the factor scores, with the highest values for Factor 5 (Sea Ice) and Factor 1 (Arctic-Greenland Waters) also occurring in this zone

(Fig. 5). Towards and across the zone 2–3 boundary, *Thalassiosira oestrupii*, *Rhizosolenia alata*, *Thalassiosira eccentrica* and *Thalassiothrix longissima* appear and increase (Fig. 2), suggesting a warming of SSTs and a reduction in the extent of seasonal ice-cover. They all prefer warmer conditions and also probably a higher salinity than in arctic conditions (Koç Karpuz & Schrader 1990; Williams 1993). This is echoed in the rapid decrease of Factor 6 (Polar Front), suggesting that the site was no longer directly influenced by Polar Waters at the end of zone 2.

Zone 3 (692.5–592.5 cm, 11 435–9240 cal. yr BP). – There are large increases in *Rhizosolenia styliformis*, *Thalassionema nitzschioides*, *Thalassiosira angulata*, *T. oestrupii* and *T. decipiens* (Fig. 2). This assemblage is typical of Factor 4 (Norwegian Atlantic Water) (Koç Karpuz & Schrader 1990) (see Appendix 3). There are also high Factor 2 scores. Towards the zone 3–4 boundary, *Rhizosolenia hebetata* var. *hebetata* and *R. hebetata* var. *semispina* increase (Fig. 2), indicating more influence of Sub-arctic Waters (see Appendix 3). At the same time, sea-ice species become rare and disappear. *Thalassiosira oestrupii* becomes abundant at the zone 3–4 boundary (Fig. 2). At the same time, Factor 3 (Sub-arctic Waters) reaches its highest levels in the sequence.

Zone 3 exhibits the highest diatom concentrations in the sequence at around $7\text{--}8 \times 10^6$ valves g^{-1} dry sediment, with peaks reaching as high as 12×10^6 valves g^{-1} dry sediment (Fig. 2).

August SST reconstructions for Zone 3 (Fig. 3) range from 11°C to 13°C. There are several short-term fluctuations of c. 1.5°C in both reconstructions. In the February SST reconstructions (Fig. 3), the temperature gently cools from c. 7°C to 9°C towards the zone 3–4 boundary with small short-term fluctuations of less than 1.0°C. A marked cooling in all reconstructions at c. 11 300–11 000 cal. yr BP is marked on Fig. 3 as 'Event a', and it can be correlated with the Pre-Boreal Oscillation (PBO) (Björck *et al.* 1997). In both February reconstructions just before a rapid warming at the zone 3–4 boundary, there is a longer cooler period (Event b) that is more marked than in the August reconstructions.

Zone 4 (592.5–452.5 cm, 9240–6550 cal. yr BP). – Zone 4 is dominated by *Thalassiosira oestrupii*, but this species decreases towards the top of the zone, while *T. eccentrica* and *Thalassionema nitzschioides* percentages increase (Fig. 2). The arctic-water species decrease above the zone 3–4 boundary. These changes suggest a major change in water-masses at the site (Fig. 5). Throughout zone 4, the ratio of *Thalassiosira gravida* spores to vegetative valves remains constant at approximately 1:1. There are individual recurrences of *Bacterosira fragilis* and *Porosira glacialis* at 540–550 cm (8190–8455 cal. yr BP) and 490 cm (7170 cal. yr BP), respectively.

There is a sharp decrease in diatom concentrations at

530–540 cm (c. 7920–8190 cal. yr BP) (Fig. 2) coincident with a sudden change at c. 540 cm (c. 8100 cal. yr BP) in the physical data (Fig. 4).

Zone 4 is dominated by Factor 2, the North Atlantic Waters. This decreases slightly towards the zone 4–5 boundary, and Factor 4, the Norwegian-Atlantic Waters, starts to increase.

This zone contains the warmest period in all the reconstructions for both August, 14°C and 15.5°C, and February, 11.5°C and 11°C, with maxima, at about 580 cm (c. 9250 cal. yr BP) (Fig. 3). The temperatures remained high until c. 7200 cal. yr BP when a cooling trend becomes apparent. There is no sign of a SST change around 540 cm parallel to the diatom concentration minimum and the changes in the physical data.

Zone 5 (452.5–320 cm, 6550–4400 cal. yr BP). – There is a steady decrease in *Thalassiosira oestrupii* percentages. Maximal percentages of *Thalassionema nitzschioides* and *Thalassiosira eccentrica* are reached and maintained throughout the rest of the sequence.

Zone 5 is the most stable zone in the sequence. All SST reconstructions (Fig. 3) show a gentle cooling trend towards the upper boundary at 320 cm (4400 cal. yr

BP). In the WA-PLS reconstruction, August SSTs cooled from 13°C to 12°C and February SSTs from 9°C to 8°C. In the I&K reconstructions, August cooled from 14°C to 12°C and February from 10°C to 8°C. There is also a steady change in the varimax factors and the inferred water-masses. Factor 2 (North Atlantic Waters) slowly decreases, whereas Factor 4 (Norwegian-Atlantic Waters) increases towards the top of the zone.

Zone 6 (320–200 cm, 4400–2665 cal. yr BP). – Zone 6 has a diatom assemblage similar to zone 5, dominated by *Thalassionema nitzschioides* (Fig. 2). *Thalassiosira oestrupii* decreases to values even lower than in zone 3, and the *T. gravis* ratios shift even further towards vegetative valves. However, zone 6 displays a sudden change in diatom assemblage around 270 cm. There is a peak of *Thalassiosira gravis* spores, increased percentages of *T. gravis* and a peak of *Rhizosolenia hebetata* var. *hebetata*, and a rise of *R. styliformis*, together with a decrease in *T. oestrupii*.

Both August SST reconstructions show a cooling trend with temperatures around 10°C continuing from zone 5 to approximately 270 cm (3660 cal. yr BP), when

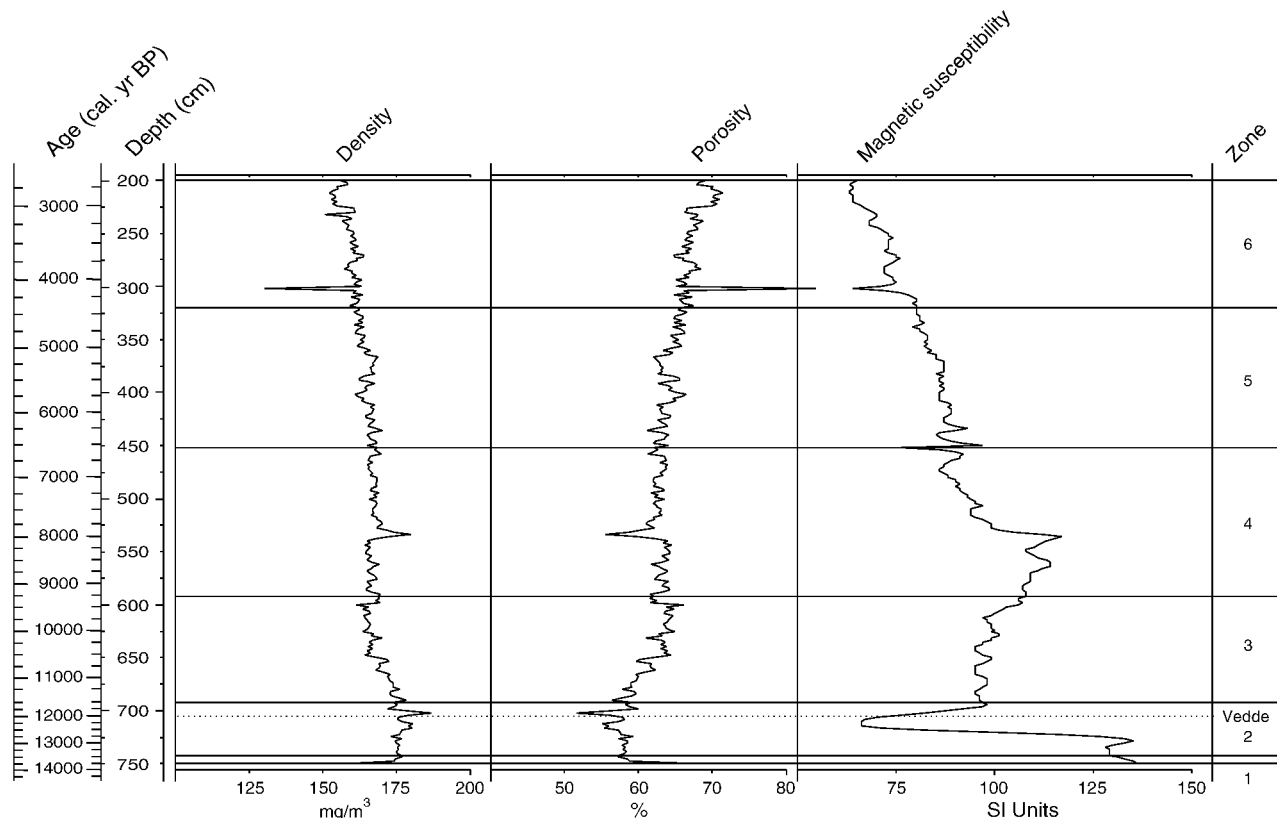


Fig. 4. Physical properties of MD95-2011 (from IMAGES 101, 1995) plotted against depth and estimated age in calibrated years BP. The magnetic susceptibility units (SI) follow IMAGES 101 (1995). The diatom assemblage zones are also shown.

the trend reversed, to show a warming to the top of zone 6 (2665 cal. yr BP), up to 12°C. The SST reconstructions for February (Fig. 3) are less consistent. I&K shows a slight warming from the minimum of 6°C at 270 cm and the greatest short-term variation. WA-PLS shows no warming, and temperature eventually falls at the top of the zone to temperatures almost as cool as the minimum at 270 cm (6°C).

Zone 6 is dominated by Factor 4 (Norwegian-Atlantic Waters), but the zone exhibits peaks in all factors except 1 and 2 (Arctic Greenland Waters and North Atlantic Waters) at 250–275 cm.

Discussion

Diatom-free levels

Diatoms are first recorded in MD95-2011 at 745 cm (c. 13 570 cal. yr BP), nearly 600 years before the first record from M23071 (Koç *et al.* 1993) from the western Vøring Plateau (Fig. 1). This may reflect a real difference in the onset of open-water conditions between the west and east sides of the Plateau, but could also be a result of poor chronologies being unable to differentiate these ages. The absence of diatoms at 715 and 720 cm (12 400 and 12 595 cal. yr BP, respectively) and 750 cm (13 765 cal. yr BP) (Fig. 2) could result from one or more of the following factors.

1. Diatoms may be dissolved in conditions of low silica-saturation combined with a slow sediment deposition rate. Post-diagenetic dissolution could also occur as bottom-water characteristics varied.
2. Diatoms are photosynthetic and at low light intensity, growth will cease. Light penetration in surface waters could be reduced by increased small-particle suspension (Sancetta 1999). If suspended particle concentration increased, the small-particle content of the sediment should also increase. This does not appear to be the case, as both the sediment density and porosity (Fig. 4) remain relatively constant during the diatom-free levels. Magnetic susceptibility falls rapidly at the upper levels, but at the lower level it shows the highest values in the sequence (Fig. 4) indicating sediment composition differences, but these were probably not related to productivity changes.
3. Ice cover also reduces light penetration and thus diatom production (Sancetta 1999; Gersonde & Zielinski 2000). The major sedimentary flux of sea-ice diatoms occurs in open water during the high-productivity summer season. During sea-ice coverage, particle flux is low and less likely to produce a signal in the diatom record. Thus the sea-ice signal is directly related to the annual duration of sea ice. For a signal to be detected, it has to persist for several years (Gersonde & Zielinski 2000). The

diatom-free levels would imply that the Vøring Plateau was covered by persistent ice for most of the year for several years. Prior to the Younger Dryas, the circulation reconstructions of Koç *et al.* (1993) suggest that the ice-margin was close to or even over the Vøring Plateau, and could have reduced diatom production before 13 570 cal. yr BP (745 cm). During the Younger Dryas, the Vøring Plateau was under an 'ice-free passage' Koç *et al.* (1993) and periodic ice-front oscillations may have affected diatoms near its margin (710–720 cm).

The ice-cover 'darkening hypothesis' is supported by reductions in primary productivity of dinoflagellates and coccoliths in the Lateglacial, in three cores from the Vøring Plateau (Baumann & Matthiessen 1992). In addition, foraminifera abundance was greatly reduced at 720 cm in MD95-2011 (Dreger 1999), suggesting a reduced overall productivity around 12 500 cal. yr BP. However, foraminifera were abundant at 755 cm (the nearest count level to the diatom-free level at 750 cm) suggesting that potential productivity was high. Therefore the most likely explanation for the low concentrations of preserved diatoms in the sediment prior to and during the Younger Dryas may be that levels of primary productivity were low due to extensive ice cover, and the valves may have been poorly preserved. If the ice-margin was near or over the Vøring Plateau, then there would be a diatom sea-ice signal, as primary production is high near ice margins.

Imbrie and Kipp Factors and water-mass interpretations

Each of the eight factors used in the I&K SST reconstructions is dominated by a particular diatom assemblage that is interpreted to represent a distinct North-Atlantic/Nordic Sea modern water-mass (Anderesen 1998; Koç Karpuz & Jansen 1992; Appendix 2). A plot of the factors against core depth (Fig. 5) reveals changes in the balance of the factors and their associated water-masses through time. These can be interpreted in terms of overall water movements and the position of the Polar Front following Koç *et al.* (1993), and summarized in Appendix 3.

As expected, not all the factors play an important role at the Vøring Plateau. Factor 1 (Arctic-Greenland Water), Factor 5 (Sea-ice Water) and Factor 8 (North Atlantic/Sub-arctic Mixing Water) all have relatively constant scores throughout the core (Fig. 5). They are present, but are not major driving factors in the SST reconstructions. However, Factors 1 and 5 have higher values below 600 cm (9420 cal. yr BP) to the base. Interestingly, Factor 5 (Sea Ice) reaches its maximum values adjacent to the 720 cm to 715 cm (12 595–12 400 cal. yr BP) diatom-free section, thus lending support to the ice-cover hypothesis as a cause for these diatom-free levels.

In zone 2 (Fig. 5), Factor 6 (Arctic Water) has the greatest weight and a strong influence on the low SST reconstructions. Such a high influence of Arctic Water suggests strongly that the Vøring Plateau was either directly below the Polar Front or very close to it during

this period. A similar conclusion was reached by Koç *et al.* (1993) and Koç & Jansen (1994). Factor 6 declined during zone 3 and became insignificant thereafter, except for a conspicuous peak in zone 6 at approximately 260 cm (3515 cal. yr BP) that reached zone 3

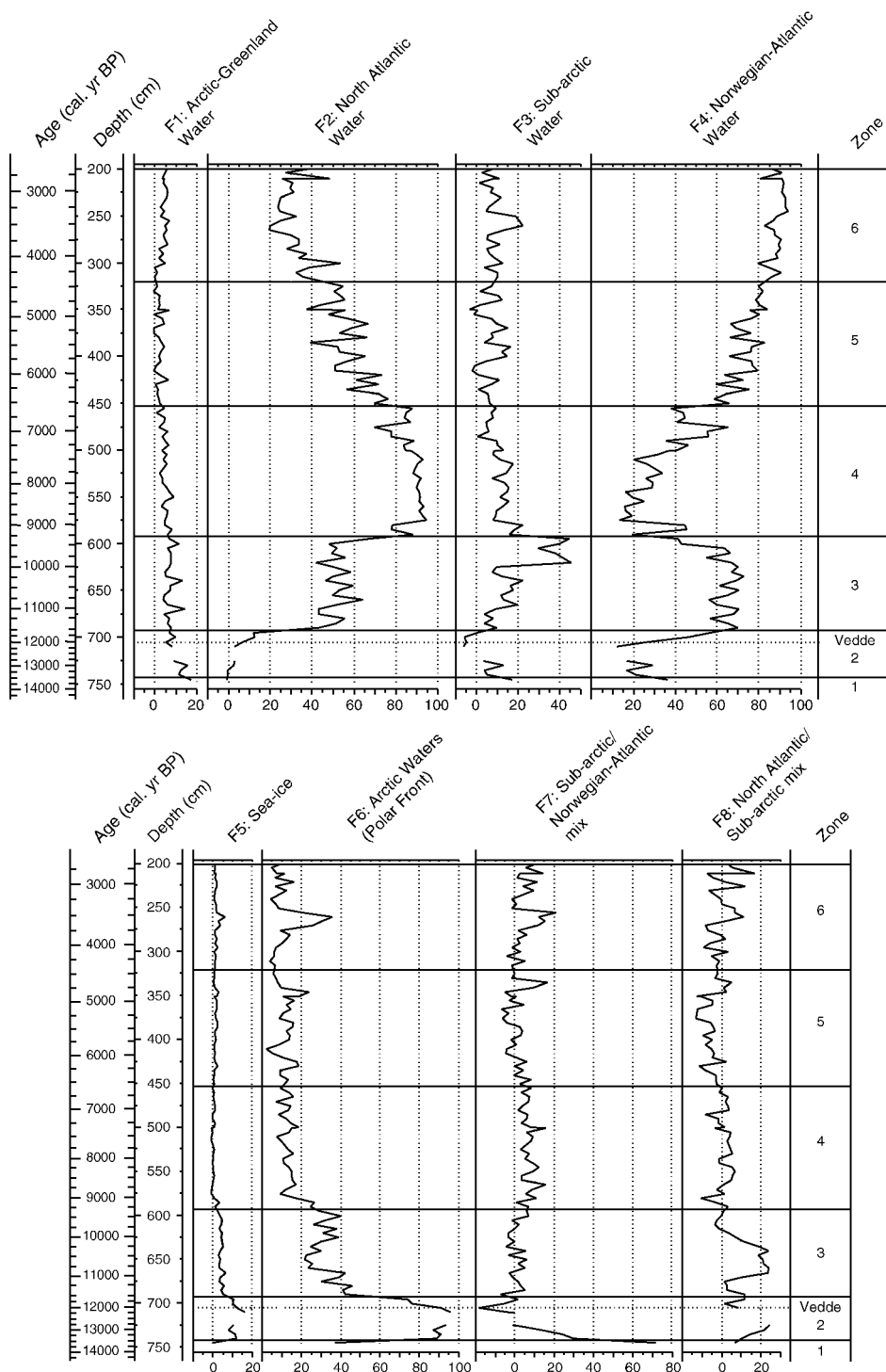


Fig. 5. Stratigraphical plot of the I&K factors ($\times 100$) interpreted as water-masses. Diatom assemblage zones are also shown, along with the estimated ages in calibrated years BP.

levels (Fig. 5). Factors 7 and 3 also peaked here, coinciding with the point where the cooling temperature trend through zones 5 and 6 reversed (Fig. 3) and SSTs started to rise.

Factor 2 (North Atlantic Water) (Fig. 5) resembles the August SST reconstruction (Fig. 3). This factor has the greatest influence on the I&K reconstructions through most of the Holocene. Factor 4 (Norwegian Atlantic Water) gradually replaced Factor 6 during zones 5 and 6, and is associated with the post-hypsithermal cooling.

Younger Dryas (12700–11550 cal. yr BP)

The diatom record at the Vøring Plateau starts between 13500 cal. yr BP (Fig. 2) and 13000 cal. yr BP (Koç *et al.* 1993). Zone 1 is dominated by a Sub-arctic/Norwegian Atlantic mix of waters (Factor 7), including Sub-arctic Waters, Norwegian Atlantic Waters, Arctic Waters and an influence of Arctic-Greenland Water (Fig. 5). Factor 2 (North Atlantic Water) increased in MD95-2011 (Fig. 5) before the Younger Dryas at the same time as the North Atlantic Factor 2 increased in the reconstruction of HM79-6/4 (Koç *et al.* 1993), suggesting that Atlantic Waters had reached the Vøring Plateau by this time. The high magnetic susceptibility (MS) values at the base of the sequence (Fig. 4) possibly reflect input of terrigenous material derived from the start of deglaciation of Norway, such as the Andøya area (Vorren *et al.* 1988). Indications of deglaciation at this time are also found in the north Norwegian Sea and the Barents Sea (Sarnthein *et al.* 1995; Hald *et al.* 1996; Hald & Aspeli 1997). The sea near southern Norway was ice-free by approximately 13400 ¹⁴C yr BP (c. 16000 cal. yr BP) (Koç Karpuz & Jansen 1992; Koç *et al.* 1993).

During the first part of the Younger Dryas (zone 2), the Vøring Plateau was subjected to the coldest temperatures in the whole of the sequence, falling to as low as 7.5°C in summer and 2.5°C in winter. Magnetic susceptibility drops to a minimum at about 12500 cal. yr BP (Fig. 4) near the chronological onset of the Younger Dryas cold episode (Björck *et al.* 1998), suggesting that there was little or no input of terrigenous material into the sediments of the Vøring Plateau during the Younger Dryas. Dokken & Jansen (1999) also found that the magnetic susceptibility signal is low during times of glacial re-advance as a result of decreased supply of material, or conditions that did not allow material to be carried far out from the Norwegian shelf, such as substantial sea-ice cover.

After this coldest spell, warming is apparent in both of the SST reconstructions, rising to between 10°C and 12°C in summer and 6°C to 8°C in winter (Fig. 3). This warming was temporarily interrupted at approximately 12000 cal. yr BP (mid-Younger Dryas). Diatom concentrations during zone 2 show a general increase towards the zone 2–3 boundary (Fig. 2). A small

interruption in this rise coincides with the cooling at 12000 cal. yr BP.

During the Younger Dryas, there was a major re-organization of water-masses at the Vøring Plateau (Fig. 5). The presence and disappearance of the Polar Front assemblages and water-masses indicate an oscillating movement of the Polar Front (Koç *et al.* 1993; Koç & Jansen 1994). Arctic Waters (representing proximity to the Polar Front) totally dominated the Vøring Plateau at MD95-2011 (Fig. 5), and the Sea ice and Greenland Waters factors reached their highest levels. During this zone, MD95-2011 was either close to, or directly under, the Polar Front. Seasonal sea ice was common, but only hindered the overall growth and production of diatoms in the early Younger Dryas (715–720 cm).

The cause of the Younger Dryas cold reversal that is so marked in the eastern North Atlantic region is still a matter of debate. Marine evidence of ice-free conditions along the whole coast of Norway as far as the Barents Sea, related to the establishment of a weak North Atlantic current circulation (Koç *et al.* 1996; Hald *et al.* 1996; Hald & Aspeli 1997) was used by Berger & Jansen (1995) to propose the 'Super Fjord Heat Pump' mechanism for climatic oscillations during deglaciation. Marked rapid coolings could be caused by substantial inflow of meltwater, which would 'cap' the warmer Atlantic Waters and promote sea-ice formation and cooling. The heat flux would be further reduced by the strong ice albedo and the prevention of surface-water currents. Because of the relatively confined geography of the Nordic Seas, rather few open areas would have occurred between ice floes to allow heat to reach the water (Copley 2000).

The distinct changes in the palaeoenvironment of the Vøring Plateau seen in the Younger Dryas SST reconstructions from MD95-2011 can be compared and correlated with records and proxies from other areas. Comparisons to other diatom-based reconstructions from the same and adjacent areas will be considered here as they show some differences and patterns (Fig. 6). The locations of these records are marked in Fig. 1. Although only the HM79-6/4 v2 reconstructions on Fig. 6 are made using the enlarged modern diatom data-set, the other curves, reconstructed on the first modern data-set (Koç Karpuz & Schrader 1990), should show comparable trends, even though the absolute temperature values may not be comparable (cf. HM79-6/4 v1 and v2).

The SST reconstructions from HM79-6/4 v1 (Koç Karpuz & Jansen 1992) show a very cold Younger Dryas at about 4°C in summer and –2°C in winter. The abrupt warming at c. 11500 cal. yr BP is interrupted by a cool event they termed YDII, before reaching mean Holocene SSTs. The new reconstruction using the enlarged modern diatom calibration set (HM79-6/4 v2, Fig. 6) indicates that the Younger Dryas was about 5°C warmer, and thus much closer to reconstructions

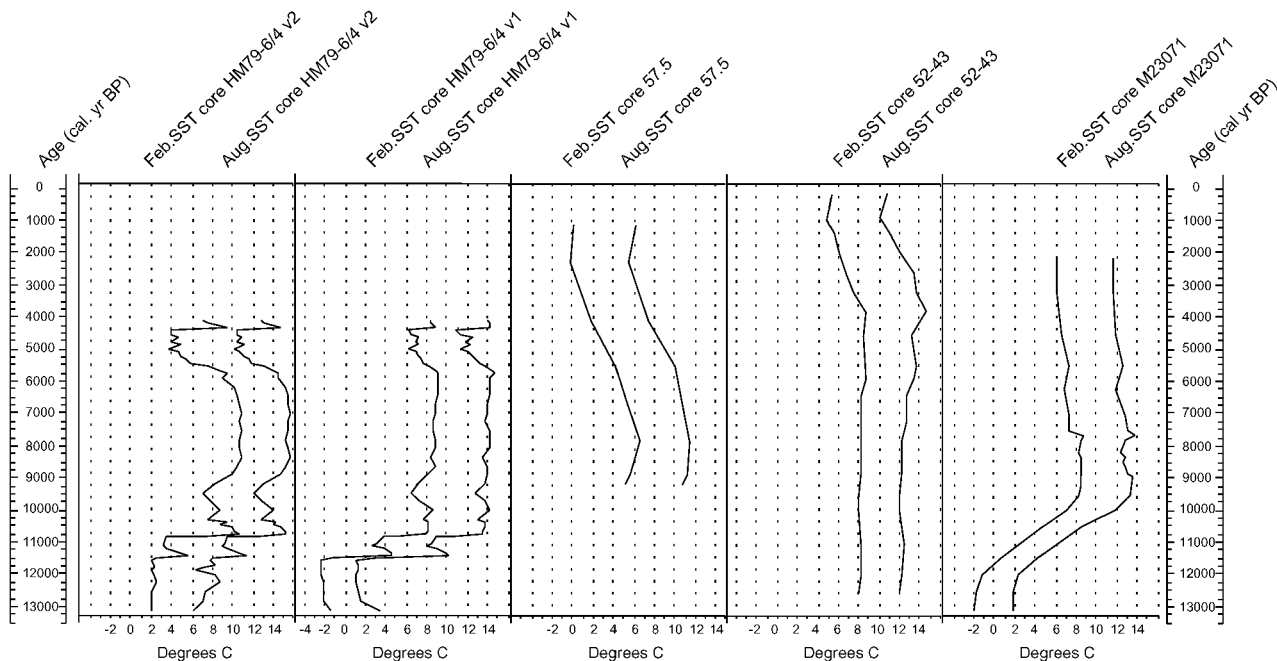


Fig. 6. Chronostratigraphical plot (calibrated years BP) of sea-surface temperature reconstructions ($^{\circ}\text{C}$) from other sites using diatoms. Core 52–43 and core 57–5 (Koç Karpuz & Schrader 1990), HM79-6/4 v1 (Koç Karpuz & Jansen 1992), core M23071 (Koç *et al.* 1993). The core locations are marked on Fig. 1. The reconstructions of HM79-6/4 v2 have been made using the enlarged calibration data-set (see text).

from MD95-2011 (Fig. 3). The site was probably ice-free during the Younger Dryas. There is less variability during the Lateglacial in HM79-6/4 v2 than HM79-6/4 v1, with the Younger Dryas to Holocene temperature increase reconstructed as a rise of 7°C rather than 9°C . However, the YDII cooling is still apparent. The SST reconstructions using the 1993 data-set from M23071, to the west of MD95-2011, are less detailed. The very cold Younger Dryas temperatures, similar to those of HM79-6/4 v1 (Fig. 6), may reconstruct warmer with the new calibration set. The early Holocene warming is gradual and shows no fluctuations. The 52–43 site (Koç Karpuz & Schrader 1990) was probably ice-free in the Younger Dryas, but the reconstructions (Fig. 6) show little temperature change.

Koç *et al.* (1993) mapped a seasonally ice-free passage to 72°N along the Norwegian coast throughout the Younger Dryas. Berger & Jansen (1995) modelled this passage as a result of a Coriolis 'pile-up' of warmer waters along the eastern side of the Nordic Sea and a weak flow of North Atlantic Waters reaching Svalbard by 13400 ^{14}C yr BP (*c.* 16000 cal. yr BP) (e.g. Koç *et al.* 1996; Hald *et al.* 1996). Koç *et al.* (1993) and Berger & Jansen (1995) also suggest that sea ice was less extensive than in the cold full glacial period before *c.* 16000 cal. yr BP.

The existence of an ice-free passage may explain the differences between MD95-2011 and M23071 (Koç *et al.* 1993) during the early Holocene and Younger Dryas

(Fig. 6). Whereas MD95-2011 is located within the northern part of the ice-free passage, M23071 may have been outside or on the edge of the passage (see Koç *et al.* (1993) Fig. 11), and may have been subjected to lengthy seasonal ice coverage, thus lowering the SST. It is important to note that the sea-ice reconstruction is based on SST estimates made with the Koç Karpuz & Schrader (1990) original modern diatom data-set. Diatom concentrations in the lower sections of MD95-2011 and M23071 show a similar trend, low numbers before and during the Younger Dryas and a steady increase during the Early Holocene (Koç *et al.* 1993), supporting the suggestion that the Younger Dryas period over the whole Vøring Plateau was cold and that surface-waters were subjected to seasonal ice-coverage.

Younger Dryas–Holocene Transition: 12000–9240 cal. yr BP

At the start of zone 3 (*c.* 12000 cal. yr BP) SSTs rose steeply. August and February SSTs both rose by $4.5\text{--}5.5^{\circ}\text{C}$ over *c.* 700 years (Fig. 3). There was a major decrease in Polar and Arctic water-masses, and a large increase in Atlantic and Norwegian-Atlantic Waters (Fig. 5). The Sea-ice assemblage was decreasing, but was still relatively high, visible by its reflection in Factor 5. The Younger Dryas/Holocene boundary

(11550 cal. yr BP) is placed at the middle of the temperature rise, at 692.5 cm.

The SST reconstructions at HM79-6/4 to the south show a rapid temperature rise at *c.* 11300 cal. yr BP which resumed after the YDII event at 9600 ¹⁴C yr BP (*c.* 10600 cal. yr BP) (Fig. 6). Core M23071 from the western Vøring Plateau shows a more gradual transition over 1500 years out of the Younger Dryas (Fig. 6). Koç *et al.* (1993) conclude that this is due '... to the much lower sedimentation rates, bioturbation effects and a larger interval of age interpolation'. However, it may also be related to the later persistence of the Polar Front over M23071 and the more gradual impact of the re-organization of the water-masses in the early Holocene than in the already ice-free passage along the Norwegian coast.

The early Holocene steep rise in temperature off the Norwegian coast and also in coastal terrestrial records at, for example, Kråkenes (Birks & Ammann 2000) can possibly be attributed to the maximum summer insolation at the time being able to warm the sea water. Most of the sea ice had melted by this time in the eastern Norwegian Sea (Koç *et al.* 1993) and was no longer reducing heat flux to the water and reflecting heat by its strong albedo (Koç *et al.* 1996). Water-mass circulation in the eastern Norwegian Sea was enhanced, probably due to enhanced overturn rates of the water column, allowing large amounts of warmer Atlantic Water to penetrate northwards up the Norwegian coast (Berger & Jansen 1995; Koç *et al.* 1996). The strong north–south gradient rapidly diminished (Koç *et al.* 1996). Diatom productivity was high over the Vøring Plateau, as shown by the rapidly increasing diatom concentrations (Fig. 2) and a parallel rise in coccolith abundances (Andruleit & Baumann 1998).

Two events can be distinguished in the SST reconstructions for zone 3 in MD95-2011 (Fig. 3). During Event a, SST fell about 1°C between 11260 cal. yr BP and 11040 cal. yr BP. Then temperatures rose to *c.* 12°C in summer and 9°C in winter. Diatom concentrations fell to a low at *c.* 11000 cal. yr BP at the end of Event a (Fig. 2) but rose swiftly to a maximum towards the top of the zone (*c.* 12×10^6 valves g^{-1} dry sediment). Event b occurred directly after Event a from 10000 cal. yr BP to the zone top at 9240 cal. yr BP. It is most marked in the winter SST, especially WA-PLS, by a sudden cooling of as much as 2°C, before temperatures started to rise again.

From its timing, Event a is likely to be related to the Pre-Boreal Oscillation (PBO) (Björck *et al.* 1996, 1997). At the same time, a similar but much more pronounced cold period, YDII, is seen in the SST records at HM79-6/4 to the south (Fig. 6) (Koç Karpuz & Jansen 1992). Comparable signals can be found on the Faeroe Isles, and can be correlated to glacial advances on Iceland (Björck *et al.* 1997), and may also possibly be reflected in the dinoflagellate, foraminifera and isotope records from Voldafjord at the

Norwegian coast (Grøsfjeld *et al.* 1999; Sejrup *et al.* 2001). Björck *et al.* (1997) suggest that the PBO was a widespread climatic cooling around the North Atlantic region. Glacial re-advances could have been initiated by decreasing summer insolation and greatly increased summer precipitation (Alley *et al.* 1993). A possible cause of the PBO could have been an increased meltwater flux into the North Atlantic from the Laurentide and Scandinavian ice sheets, along with the sudden influx of fresh waters from the Baltic Ice Lake (Björck *et al.* 1996; Hald & Hagen 1998; Sejrup *et al.* 2001) that slowed or decreased the thermohaline circulation, and in addition would have had a positive feedback on ocean cooling by the formation of sea ice, as earlier at the onset of the Younger Dryas. Thus one would expect a southerly displacement of the Polar Front, and a cooling of the North Atlantic. The cooling in Event a, correlated with the PBO, involved an increase in Factor 6 (Arctic Waters – Polar Front, Fig. 5). During the time of Event b (Fig. 3), there was a period of glacial equilibrium line altitude (ELA) depressions and glacial re-advance on Iceland and in western Norway at approximately 10600 cal. yr BP (Fig. 7). However, there is no signal in the Sea-ice Factor (5 in Fig. 5) over the Vøring Plateau. It seems likely that warm North Atlantic Water promoted ice-sheet melting, but the consequent increase in the Norwegian coastal current and glacial meltwater input slowed the thermohaline circulation leading to renewed cooling. Equilibrium had not yet been reached.

Holocene maximum warmth: 9240–6750 cal. yr BP

A small cooling of up to 2°C between 9500 and 9300 cal. yr BP breaks the warming trend following Event b (Fig. 3). The warming trend then continued and warm waters were passing over the Vøring Plateau and reaching as far north as Svalbard (e.g. Salvigsen *et al.* 1992), creating the warmest climatic conditions between 8700 and 7700 ¹⁴C BP (*c.* 7650–6500 cal. yr BP).

Throughout the Holocene, summer SST reconstructions show small fluctuations, but the trends are clear (Fig. 3). Both reconstructions show a clear period of maximum mean temperatures between 9000 cal. yr BP and 6750 cal. yr BP (corresponding roughly with zone 4). The maximum summer temperatures between 13°C and 15°C and winter temperatures of up to 11°C (Fig. 3) were almost 4°C warmer than present temperatures over the Vøring Plateau (*c.* 11°C and 7°C, respectively – Hopkins 1991).

The Holocene SST reconstructions from the Norwegian Sea (Fig. 1) are compared in Fig. 6. Up to about 5000 ¹⁴C yr BP (5700 cal. yr BP), cores 52–43 (Koç Karpuz & Schrader 1990) and HM79-6/4 (Koç Karpuz & Jansen 1992) both show stable summer SSTs, and similar winter temperatures. However, the new reconstruction of HM79-6/4 SSTs (v2) (Fig. 6) shows a

record of temperature range and change that is closer to MD95-2011 (Fig. 3). The curves show a similar period of maximum temperature of about 15°C at almost the same time as in MD95-2011 (c. 8500 cal. yr BP). Core M23071 from the western Vøring Plateau also shows a generally similar period of maximum warmth to MD95-2011 followed by a gentle decrease of c. 1.5°C up to its top at about 2200 cal. yr BP. However, the temperature values are lower by about 1–2°C than MD95-2011 and HM79-6/4 v1 and v2, but are still about 1°C higher than core 52–43, and the amplitude of change is also smaller. The record from 52–43, lying between MD95-2011 and HM79-6/4 (Fig. 1), is rather different (Fig. 6), with constant SSTs at c. 12 and 8°C from c. 12500–8000 cal. yr BP that rose slowly to a maximum of 15 and 9°C at c. 3800 cal. yr BP and then declined to a minimum at c. 1000 cal. yr BP. It is possible that reconstructions of the 52–43 data with the enlarged modern calibration data-set may change the values. Core 57–5 from the Iceland Sea (Koç Karpuz & Schrader 1990) shows a similar pattern to M21073 from the western Vøring Plateau, with a period of maximum warmth between 9000 ¹⁴C yr BP and 6000 ¹⁴C yr BP (9900 cal. yr BP and 6800 cal. yr BP), similar in timing to the warmth maximum in the northern Norwegian Sea (Hald *et al.* 1996), a temperature maximum near 7000 ¹⁴C yr BP (c. 7800 cal. yr BP), and a low range of variability. The temperatures near Iceland were lower overall by about 2°C compared to the Norwegian Basin, and the difference was greater in winter than in summer.

Similar trends were shown by foraminiferal reconstructions made by Eiriksson *et al.* (2000) from that area.

As discussed by Koç *et al.* (1993), times of maximum temperatures vary between the sites. MD95-2011 reached a maximum Holocene temperature of c. 15°C at about 8500 cal. yr BP followed by a gradual decline to a minimum at around 3500 cal. yr BP (Fig. 3). Core 52–43 (Koç Karpuz & Schrader 1990) reached a maximum temperature of over 14°C much later, at c. 3800 cal. yr BP before decreasing to a minimum at c. 1000 cal. yr BP (Fig. 6). Core HM79-6/4 shows a very slight SST increase from the early Holocene up to a maximum of over 14°C at c. 5700 cal. yr BP, followed by a marked temperature drop to about 12°C at c. 4700 cal. yr BP, which it maintained for c. 600 years when there was an abrupt rise back to over 14°C.

Koç *et al.* (1993, 1996) comment that the ice-free passage along western Norway had expanded sufficiently to allow warm waters to reach Svalbard around 9000 ¹⁴C yr BP (c. 9900 cal. yr BP, with optimal climatic conditions being reached between 8700 and 7700 ¹⁴C yr BP (c. 7650–6500 cal. yr BP). Thermophilous molluscs were present near Svalbard (Salvisgen *et al.* 1992) and Atlantic Water predominated in the Barents Sea (Duplessy *et al.* 2001). Foraminiferal analyses by Hald *et al.* (1996) and Hald & Aspeli (1997) reconstruct SSTs warmer than present-day conditions in the north Norwegian Sea. Temperature reconstructions from pollen data in NW Finland (Seppä & Birks 2000) also show a period of maximum warmth

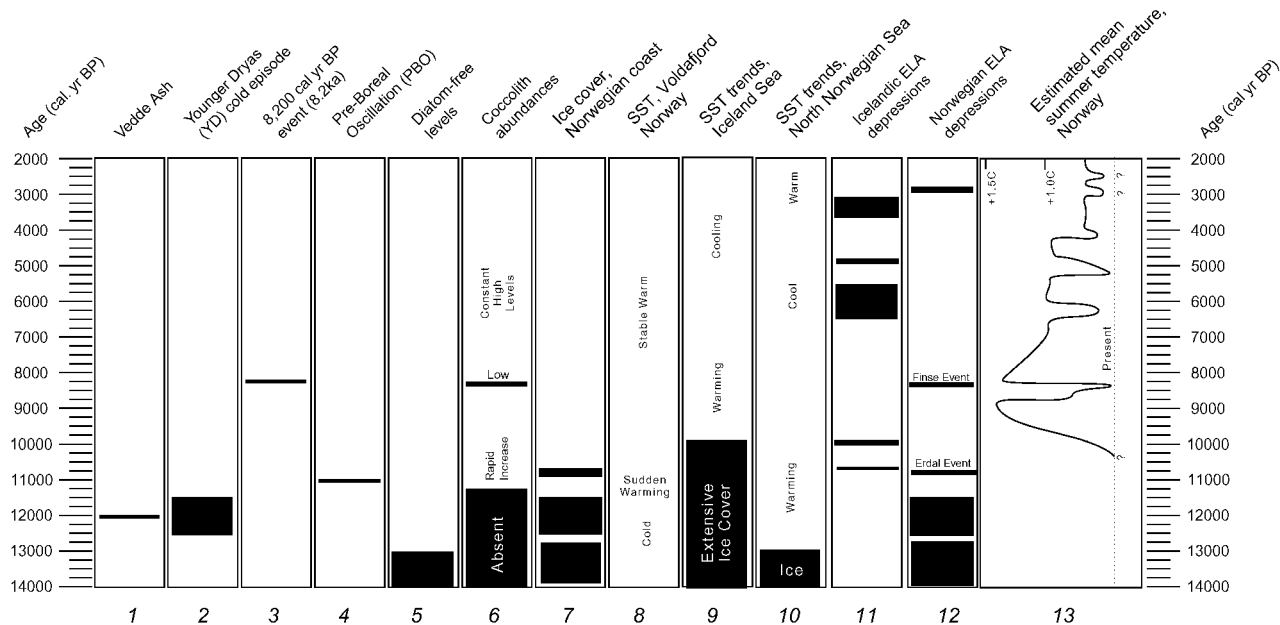


Fig. 7. Chronological comparison chart of climatic events described from the Norwegian Sea region. 1. Grønvald *et al.* (1995); 2. Björck *et al.* (1998); 3. Alley *et al.* (1997); 4. Björck *et al.* (1997); 5. Koç *et al.* (1993); 6. Baumann & Matthiessen (1992); 7, 8. Grøsfjeld *et al.* (1999), Sejrup *et al.* (2001); 9. Eiriksson *et al.* (2000); 10. Hald & Aspeli (1997); 11. Stötter *et al.* (1999); 12, 13. Nesje & Dahl (1993), Dahl & Nesje (1996).

between *c.* 8000 and 6750 cal. yr BP. By comparison, the SST record from MD95-2011 far to the south shows that the warmest period in the reconstruction was earlier and longer between 9500 cal. yr BP and 7500 cal. yr BP, which suggests a lag of about 500 years in the warming in the north (see Koç *et al.* 1996).

Koç *et al.* (1993) interpret a time-transgressive migration of diatom assemblages to the north and west of the Nordic Seas during the early Holocene as the north-westward migration of the Polar Front. The reconstructions from MD95-2011 support this interpretation. Koç *et al.* (1993) also note that changes in diatom concentrations are paralleled in the coccolith and dinoflagellate records of Baumann & Matthiessen (1992). From their data, Koç *et al.* (1993) propose that the Arctic front migrated to the west of Iceland by 9000 ¹⁴C yr BP (*c.* 10000 cal. yr BP), and that there was little change in the mean position of the Arctic Front from 9000 ¹⁴C yr BP to 5000 ¹⁴C yr BP (*c.* 10000 cal. yr BP to 5700 cal. yr BP). As mentioned above, Factor 6 that is connected to the Polar Front, decreased in MD95-2011 from *c.* 12000 cal. yr BP (Fig. 5), but it exhibited a peak between 10500 cal. yr BP and 9500 cal. yr BP, that probably corresponds with the final migration of the Polar Front from the Vøring Plateau area.

The first half of the Holocene was the period of greatest influence of the Atlantic Waters over the Vøring Plateau. Atlantic-Water dominance is only challenged by a gradual increase in Norwegian-Atlantic Waters after about 7500 cal. yr BP (Factor 4; Fig. 5). After 7700 cal. yr BP, Grøsfjeld *et al.* (1999) show that the Norwegian Coastal current was also starting to build in strength.

The 8200 cal. yr BP event

A transient climatic cooling about 8200 calibrated years ago (8.2 ka BP) inferred from Greenland ice cores (e.g. Dansgaard 1987; Alley *et al.* 1997) has been widely correlated with climatic records from other regions (e.g. O'Brien *et al.* 1995; Alley *et al.* 1997; Klitgaard-Kristiansen *et al.* 1998; Duplessy *et al.* 2001). Its cause has been proposed as a cold meltwater plume that entered the North Atlantic from the catastrophic drainage of pro-glacial lakes of the Laurentide Ice Sheet, causing a short-lived cooling and freshening of the surfaces and a slowing of the thermohaline circulation (e.g. Barber *et al.* 1999; Renssen *et al.* 2001).

At 540 cm in MD95-2011, age-modelled to *c.* 8100 cal. yr BP, diatom concentrations fluctuating between 6 and 9×10^6 valves g^{-1} dry sediment crash to less than 3×10^6 valves g^{-1} dry sediment (Fig. 2). Concentrations subsequently recovered to about 4×10^6 valves g^{-1} dry sediment but the early Holocene concentrations were not regained until the top of the sequence at 210 cm (2805 cal. yr BP). Also at 540 cm (*c.* 8100 cal. yr BP), all three records of physical data from MD95-2011 show a simultaneous peak (Fig. 4) suggesting a

transient change in sediment composition. However, a rapid, short-term cooling at *c.* 8200 cal. yr BP (e.g. Klitgaard-Kristiansen *et al.* 1998) is not distinct in the diatom-based temperature reconstructions (Fig. 3) where there are many minor fluctuations, although the largest temperature dip in reconstructions made using the modern analogue technique occurs at exactly this time (Birks 2001). The 5 cm sample-resolution of the diatom record in MD95-2011 (*c.* 90 years) may not be fine enough to detect any 8.2 ka event itself, but the generally fluctuating SSTs over this period suggest instability in the distribution of the main water-masses and the sensitivity of the thermohaline circulation to influxes of glacial meltwater, as suggested by Alley *et al.* (1997), Keigwin & Jones (1995), Hu *et al.* (1999) and Renssen *et al.* (2001), perhaps responding to drainage of other glacial lakes and ice-sheet melting in the North Atlantic region (e.g. Hu *et al.* 1999). The final melting of the Norwegian ice sheet (*c.* 8000 ¹⁴C yr BP, *c.* 8700 cal. yr BP: Nesje & Dahl 1993) also occurred around this time.

However, the crash in total diatom concentration is marked, and could possibly be due to a change in the water-masses that decimated the diatom population but did not cause any prolonged fluctuation in SST. Diatom concentrations may also have been affected by chemical changes in an abrupt modification of the surface waters, such as waters significantly undersaturated with silica, or waters containing fewer nutrients. Such changes would permit fewer valves to be preserved on the sea floor but not substantially change the relative composition of the fossil assemblage.

Between 550 cm and 540 cm there are minor occurrences of *Bacterosira fragilis* (Fig. 2), a cold-water species (Koç Karpuz & Schrader 1990). The August SSTs at this time were between 12°C and 15°C in this and nearby cores (e.g. Figs 3 and 6), so the presence of this diatom could be explained by long-distance transport in drift ice or the water column from the Greenland/Labrador Seas, perhaps even from the 8.2 ka BP event itself. This hypothesis is supported by the small peak of Factor 1 (Arctic-Greenland Water) between 545 and 555 cm (*c.* 8100 cal. yr BP) (Fig. 5).

Besides the reduced diatom concentration, some other permanent changes occurred after *c.* 8100 cal. BP at the Vøring Plateau. The magnetic susceptibility curve declined rapidly (Fig. 4) suggesting a change in sedimentary composition. The Laurentide drainage would have forced a reorganization of the oceanic currents, and thus a change in the primary source of material being deposited on the Vøring Plateau. Fig. 5 indicates the start of a steady increase in Norwegian Atlantic Water at the expense of North Atlantic Water at this time, which could account for the sedimentary change. A greatly reduced amount of material was transported from Iceland after this reorganization, thus leading to a lower iron content in the sediments, and a lower MS curve (E. Jansen, pers. comm. 2001).

Holocene cooling: 6550–3500 cal. yr BP

The MD95-2011 record shows that waters over the Vøring Plateau cooled from *c.* 7230 cal. yr BP (Fig. 3) at a rate of approximately 1°C every 1000 years in the summer SST record. The trend lasted for almost 3700 years, until 3500 cal. yr BP, and encompassed a drop in temperatures of almost 5°C in summer and 4°C in winter to lows of approximately 10°C in summer and 6°C in winter. Diatom concentrations (Fig. 2) were around 4×10^6 valves g^{-1} dry sediment with a minimum at *c.* 5000 cal. yr BP of 2×10^6 valves g^{-1} dry sediment. In HM79-6/4 (Koç Karpuz & Jansen 1992) to the south, minimum concentration occurred at 4500 cal. yr BP, suggesting a time-transgressive change. Diatom concentration peaks in HM79-6/4 are dominated by large numbers of *Chaetoceros* spores (Koç Karpuz & Jansen 1992), suggesting a combination of high productivity and upwelling (Williams 1986; Koç Karpuz & Schrader 1990; De Sève 1999). Similarly, productivity varied through zone 5 at MD95-2011 (Fig. 2), increasing irregularly after the minimum until *c.* 3000 cal. yr BP, when there was a large rapid increase.

The overall cooling is marked by many small temperature fluctuations in the high resolution record of MD95-2011, mostly less than 1°C. The most prominent small coolings appear at *c.* 6250 cal. yr BP, *c.* 5500 cal. yr BP, *c.* 5000 cal. yr BP, *c.* 4500 cal. yr BP, and *c.* 3500 cal. yr BP. Minimum temperatures were reached at 3515 cal. yr BP, the most prominent of the late-Holocene short-term coolings. Two periods of ELA depression on Iceland at 6600–5500 cal. yr BP and at 4600 cal. yr BP, probably resulting from increased precipitation combined with cooler conditions (Stötter *et al.* 1999), can be tentatively correlated to the small dips in the SST records, especially the Bægisádalur I advance at 4600 cal. yr BP (Fig. 7). Glaciers redeveloped in western Norway at about 5100 ^{14}C yr BP (*c.* 6000 cal. yr BP) (Nesje & Dahl 1993; Dahl & Nesje 1996), a similar time to glacial re-advance in Iceland (Stötter *et al.* 1999). Temperature reconstructions from pollen data in NW Finland and other terrestrial records in northern Norway all indicate the onset of cooling after the mid-Holocene period of maximum warmth at around 6500 cal. yr BP (Seppä & Birks 2000). The increasing dominance of Norwegian-Atlantic Water during zone 5 (Fig. 5) probably reinforced the gentle cooling trend and supplied increasingly moist air-masses to the Norwegian mountains and to Iceland. Terrestrial conditions may have been becoming colder as summer insolation was decreasing and the SST of the Vøring Plateau was falling.

Compared with the gradually falling temperatures after 6750 cal. yr BP in MD95-2011 (Fig. 3), in core M23071 the cooling was slight, and in core 52–43 it did not even start until *c.* 4000 cal. yr BP (Fig. 6). In contrast, cooling was at least 6°C in core 57–5 from the

Iceland Plateau, following the pattern in M23071, until *c.* 1350 cal. yr BP (Koç Karpuz & Schrader 1990). A similar trend can be seen in foraminiferal reconstructions from the Iceland Sea from 6500–3500 cal. yr BP (Eiríksson *et al.* 2000). In HM79-6/4 the pattern appears different, but the record stops at approximately 3800 cal. yr BP. After a period of constant temperature, it shows an increased rate of cooling from 6750 cal. yr BP towards 4750 cal. yr BP and a distinct cool period at about 11°C in summer until 4000 cal. yr BP, followed by a rapid warming back to 14°C (Fig. 6).

The displacement of the Atlantic Waters continued through zones 5 and 6, resulting in declines in the reconstructed SSTs. The gradual cooling is related to the decrease in summer insolation in the northern hemisphere. Sea ice increased in the west after *c.* 7000 cal. yr BP (Koç *et al.* 1993; Eiríksson *et al.* 2000), increasing the albedo and reducing heat flux, and promoting further ice formation as a positive feedback (Copley 2000). However, thermohaline circulation was not diminished (Koç *et al.* 1996), but water-masses were gradually re-organized until Norwegian-Atlantic Water became the dominant water-mass at the Vøring Plateau with North Atlantic Water greatly reduced (Fig. 5). There are peaks in several water-mass indicators at 260 cm (*c.* 3500 cal. yr BP), including a small peak in the sea-ice factor (Factor 5) and a large peak in the Arctic Waters factor (Factor 6) corresponding to the temperature minimum (Fig. 5).

Late Holocene warming: from c. 3500 cal. yr BP

Following the temperature minimum in MD95-2011, a warming trend continued to the top of the sequence. The SST of the Vøring Plateau rose by about 2°C in summer and 1°C in winter by 2665 cal. yr BP. While temperatures were rising in the east, temperatures were still falling slightly in cores M23071 in the west, 52–43 to the south, and 57–5 from the Iceland Sea. They rose subsequently at around 1000 cal. yr BP. Temperatures in HM79-6/4 even further south had risen abruptly after the cool period, but then the record ceases. A mechanism for increased ocean temperature occurring at the same time as decreasing terrestrial temperatures is proposed by Hald & Aspeli (1997). Warm ocean temperatures result from an increased strength of the Gulf Stream promoted by low pressure atmospheric conditions that cause wet and cold conditions on land.

Comparison of different palaeo-records

Two major problems in comparing marine records are (1) the construction of reliable chronologies from material that is often difficult to radiocarbon date, and with poorly constrained tephra horizons, and (2) the difficulty of comparing marine, terrestrial, and ice-core calendar ages due to the relatively poorly known marine

reservoir effect, especially in the Lateglacial (Lowe *et al.* 2001).

Differences between the diatom-inferred SST results of Koç Karpuz & Schrader (1990), Koç Karpuz & Jansen (1992), Koç *et al.* (1993) and those presented from MD95-2011 can be interpreted as the sites (Fig. 1) experiencing different patterns of Holocene current development in space and time as water-masses were diverted or displaced locally by other water-masses or areas of sea-ice. However, poor dating and chronology, along with local changes in sedimentary conditions could also introduce inconsistencies between sites. Local conditions may also have influenced diatom preservation through re-deposition, dissolution or retarded deposition. A methodological factor that influences site differences in SST is the evolution of the Nordic Seas modern diatom calibration set, as more modern surface samples with modern SST data have been added to the data-set after 1993. As shown by the I&K reconstructions of HM79-6/4, v1 and v2, the SST reconstructions using the same diatom stratigraphical data show some differences, as the reconstructions are inevitably influenced by the range of modern temperatures in the modern training set used (see Birks 1998). Because modern diatom samples from warmer waters are included in the enlarged data-set, higher temperatures are reconstructed. The use of the enlarged data-set on HM79-6/4 v2 results in often warmer SST reconstructions and the differentiation of a hypsithermal interval in the early Holocene comparable to that seen in MD95-2011. Small differences in diatom taxonomy may have played a role in the different SST reconstructions between sites, although Birks (2001) demonstrated that this makes an insignificant difference to the SST reconstructions. Direct comparisons between sites must be made with these possible methodologically induced differences in mind.

If the differences between sites are real, then spatial patterns at different times can be detected and mapped (e.g. Koç *et al.* 1993; Koç & Jansen 1994; Koç *et al.* 1996) and related to changes in other proxy records both from land and the sea in an attempt to understand the mechanisms and changes in the earth-climate system in the past. Obviously, deductions about temporal and spatial changes in the SSTs and ocean water-masses will be strengthened if all the compared records are made on the same basis. The results from MD95-2011 have added high-resolution information on oceanographic and climatic changes from a sensitive area of the Norwegian Sea that can contribute to the building of a larger synthetic picture of lateglacial and Holocene palaeoclimatic and palaeoceanographic conditions.

Concluding remarks

The North Atlantic has been subjected to marked climatic changes since the last glacial. The heat fluxes

to the northerly region and its surrounding land masses are intrinsically linked. During the Younger Dryas, the North Atlantic was dominated by cold, arctic waters, and sea-ice was common. After the cold Younger Dryas with summer SSTs about 6–7°C, temperatures warmed rapidly in the Holocene to about 13°C, as the warmer North Atlantic Current gained in strength. This allowed productivity of both diatoms and other primary producers to increase. During this warming, there were small fluctuations in the SST record, some of which can be correlated to terrestrial records. A fluctuation in the earliest Holocene can be related to the Pre-Boreal Oscillation, but sea-surface temperatures were generally unstable until about 9700 cal yr BP. Evidence from diatom concentrations and magnetic susceptibility suggests a change and stabilisation of water currents associated with the final melting of the Scandinavian ice sheets and Laurentide ice sheets at *c.* 8100 cal yr BP. A period of maximum warmth between 9700 and 6700 cal yr BP had sea-surface temperatures 3–5°C warmer than at present. Temperatures cooled gradually until *c.* 3000 cal yr BP, and then they rose slightly around 2750 cal yr BP. Since about 7250 cal yr BP, Norwegian Atlantic Water has gradually replaced the North Atlantic Water, and in combination with decreasing summer insolation, has led to the gradual cooling of the sea surface. Terrestrial systems in Norway and Iceland have responded to the cooling and the increased supply of moisture by renewed glaciation. Periods of glacial advance can be correlated with cool oscillations in the sea-surface temperature reconstructions. By comparison with records of sea-surface temperatures from other sites in the Norwegian Sea, spatial and temporal changes in patterns of ocean water-masses have been reconstructed, demonstrating a complex system of feedbacks and influential factors in the climate of the North Atlantic and Norway.

Acknowledgements. – This manuscript has benefited greatly from comments by Carin Andersson, Hilary Birks, John Birks, Holger Cremer, Jan Piotrowski, Eystein Jansen, and an anonymous reviewer, and from additional discussions with Svein Olaf Dahl, Atle Nesje, and Bjørg Risbrobakken. John Birks, Cajo ter Braak, Steve Juggins, and John Line have allowed us to use unpublished computer software. Trond Dokken established the stratigraphic position of the Vedde Ash in our core. Sylvia Peglar has provided invaluable assistance with Figure 2. The work has been supported by the following bodies: Norwegian Research Council (NFR) 133455/720 'Holocene heat flux variability'; L. Meltzers Høyskolefond (1997); EC Environmental Project 'Holocene Ocean Instability'; and Nordic Ministers Arctic Programme 'POLARCLIM'. We are most grateful to all these people and institutions.

References

- Alley, R. B., Meese, D. A., Shuman, C. A., Gow, A. J., Taylor, K. C., Grootes, P. M., White, J. W., Ram, M., Waddington, E. D., Mayewski, P. A. & Zielinski, G. A. 1993: Abrupt increase in Greenland snow accumulation at the end of the Younger Dryas event. *Nature* 362, 527–529.

- Alley, R. B., Mayewski, P. A., Sowers, T., Stuiver, M., Taylor, K. C. & Clark P. U. 1997: Holocene climatic instability: A prominent, widespread event 8200 years ago. *Geology* 25, 483–486.
- Andersen, C. 1998: *Studier av klimavariabilitet i De Nordiske Hav og Danmarkstredet med hovedvekt på de siste 2000 år, basert på diatomésammensetninger i marine kjerne*. M.Sc. thesis, University of Bergen, Norway, 118 pp.
- Andrulleit, H. A. & Baumann, K. 1998: History of the last deglaciation and Holocene in the Nordic seas as revealed by coccolithophore assemblages. *Marine Micropaleontology* 35, 179–201.
- Barber, D. C., Dyke, A., Hillaire-Marcel, C., Jennings, A. E., Andrews, J. T., Kerwin, M. W., Bilodeau, G., McNeely, R., Southon, J., Morehead, M. D. & Gagnon, J.-M. 1999: Forcing of the cold event of 8200 years ago by catastrophic drainage of Laurentide lakes. *Nature* 400, 344–348.
- Baumann, K. H. & Matthiessen, J. 1992: Variations in surface-water mass conditions in the Norwegian Sea: Evidence from Holocene coccolith and dinoflagellate cyst communities. *Marine Micropaleontology* 35, 215–240.
- Bennett, K. D. 1996: Determination of the number of zones in a biostratigraphical sequence. *New Phytologist* 132, 155–170.
- Berger, W. H. & Jansen E. 1995: Younger Dryas episode: ice-collapse and super-fjord heat pump. In Troelstra, S. R., van Hinte, J. E. & Ganssen, G. M. (eds.): *The Younger Dryas*, 61–105. Proceedings of the Royal Dutch Academy of Natural Science 44.
- Birks, C. J. A. 2001: *A Younger Dryas–Holocene diatom record of sea-surface temperatures and oceanographic changes from core MD95-2011, Vøring Plateau*. M.Sc. thesis, University of Bergen, 171 pp.
- Birks, H. H. & Ammann, B. 2000: Two terrestrial records of rapid climate change during the glacial-Holocene transition (14000–9000 BP) from Europe. *Proceedings National Academy of Sciences USA* 97, 1390–1394.
- Birks, H. H., Battarbee, R. W. & Birks, H. J. B. 2000: The development of the aquatic ecosystem at Kråkenes Lake, western Norway, during the late-glacial and early Holocene—a synthesis. *Journal of Paleolimnology* 23, 91–114.
- Birks, H. H., Gulliksen, S., Hafliðason, H. & Mangerud, J. 1996: New radiocarbon dates for the Vedde Ash and the Saksunarvatn Ash from western Norway. *Quaternary Research* 45, 119–127.
- Birks, H. J. B. 1995: Quantitative palaeoenvironmental reconstructions. In Maddy, D. & Brew, J. S. (eds.): *Statistical Modelling of Quaternary Science Data. Technical Guide 5*, 161–254. Quaternary Research Association, Cambridge.
- Birks, H. J. B. 1998: D. G. Frey and E. S. Deevey Review #1. Numerical tools in palaeolimnology - Progress, potentialities, and problems. *Journal of Paleolimnology* 20, 307–332.
- Birks, H. J. B. & Gordon, A. D. 1985: *Numerical methods in Quaternary pollen analysis*. 317 pp. Academic Press, London.
- Björck, S., Kromer, B., Johnsen, S., Bennike, O., Hammarlund, D., Lemdahl, G., Possnert, G., Rasmussen, T. L., Wohlfarth, B., Hammer, C. U. & Spurk, M. 1996: Synchronized terrestrial-atmospheric deglacial records around the North Atlantic. *Science* 274, 1155–1160.
- Björck, S., Rundgren, M., Ingólfsson, Ó. & Funder, S. 1997: The Preboreal oscillation around the Nordic Seas: terrestrial and lacustrine responses. *Journal of Quaternary Science* 12, 455–465.
- Björck, S., Walker, M. J. C., Cwynar, L. C., Johnsen, S., Knudsen, K.-L., Lowe, J. J., Wohlfarth, B. & INTIMATE members 1998: An event stratigraphy for the Last Termination in the North Atlantic region based on the Greenland ice-core record: a proposal by the INTIMATE group. *Journal of Quaternary Science* 13, 283–292.
- ter Braak, C. J. F. 1995: Non-linear methods for multivariate statistical calibration and their use in palaeoecology: a comparison of inverse (k - nearest neighbours, partial least squares and weighted averaging partial least squares) and classical approaches. *Chemometrics and Intelligent Laboratory Systems* 28, 165–180.
- ter Braak, C. J. F. & Juggins, S. 1993: Weighted averaging partial least squares regression (WA-PLS): an improved method for reconstructing environmental variables from species assemblages. *Hydrobiologia* 269/270, 485–502.
- ter Braak, C. J. F., Juggins, S., Birks, H. J. B. & van der Voert, H. 1993: Weighted averaging partial least regression (WA-PLS): definition and comparison with other methods for species-environment calibration. In Patil, G. P. & Rao, C. R. (eds.): *Multivariate Environmental Statistics*, 525–560. Elsevier Science Publishers, Amsterdam.
- Bradley, R. S. 1999: Marine Sediments and Corals. In Bradley, R. S. (ed.): *Paleoclimatology: Reconstructing Climates of the Quaternary*, 191–280. Harcourt Academic Press, San Diego.
- Broecker, W. S. 1991: The great ocean conveyor. *Oceanography* 4, 79–89.
- Copley, J. 2000: The great ice mystery. *Nature* 408, 634–636.
- Dahl, S. O. & Nesje, A. 1996: A new approach to calculating Holocene winter precipitation by combining glacier equilibrium-line altitudes and pine-tree limits: a case study from Hardangerjøkulen, central Norway. *The Holocene* 6, 381–398.
- Damuth, J. E. 1978: Echo relationships of the Norwegian-Greenland Sea: relationship to Quaternary sedimentation. *Marine Geology* 28, 1–36.
- Dansgaard, W. 1987: Ice core evidence of abrupt climatic changes. In Berger, W. J. & Labeyrie, L. D. (eds.): *Abrupt Climatic Change: Evidence and Implications*, 223–233. Reidel, Dordrecht.
- De Sève, M. 1999: Transfer function between surface sediment diatom assemblages and sea-surface temperature and salinity of the Labrador Sea. *Marine Micropaleontology* 36, 249–267.
- Dokken T. M. & Jansen, E. 1999: Rapid changes in the mechanism of ocean convection during the last glacial period. *Nature* 401, 458–461.
- Dreger, D. 1999: *Decadal-to-centennial-scale sediment records of ice advance on the Barents shelf and melt-water discharge onto the North-eastern Norwegian Sea over the last 40 Kyr*. Ph.D. dissertation, University of Kiel, 80 pp.
- Duplessy, J.-C., Ivanova, E., Murdmaa, I., Paterne M. & Labeyrie, L. 2001: Holocene paleoceanography of the northern Barents Sea and variations of the northward heat transport by the Atlantic Ocean. *Boreas* 30, 2–16.
- Eiriksson, J., Knudsen, K. L., Hafliðason, H. & Henriksen, P. 2000: Late-glacial and Holocene paleoceanography of the North Iceland Shelf. *Journal of Quaternary Science* 15, 23–42.
- Gersonde, R. & Zielinski, U. 2000: The reconstruction of late Quaternary Antarctic sea-ice distribution - the use of diatoms as a proxy for sea-ice. *Palaeogeography, Palaeoclimatology, Palaeoecology* 162, 263–286.
- Grimm, E. C. 1990/1991: TILIA and TILIA-GRAPH software for handling and plotting pollen stratigraphical data. Illinois State Museum, Springfield, Illinois.
- Grønvald, K., Óskarsson, N., Johnsen, S. J., Clausen, H. B., Hammer, C., Bond, G. & Bard, E. 1995: Ash layers from Iceland in the Greenland GRIP ice core correlated with oceanic and land sediments. *Earth and Planetary Science Letters* 135, 149–155.
- Grøsfjeld, K., Larsen, E., Serjup, H. P., de Vernal, A., Flatebø, T., Vestbø, M., Hafliðason, H. & Aarseth, I. 1999: Dinoflagellate cysts reflecting surface-water conditions in Voldafjorden, western Norway during the last 11,300 years. *Boreas* 28, 403–415.
- Gulliksen, S., Birks, H. H., Possnert, G. & Mangerud, J. 1998: A calendar age estimate of the Younger Dryas - Holocene boundary at Kråkenes, western Norway. *The Holocene* 8, 249–259.
- Hafliðason, H., Eiriksson, J. & van Kreveld, S. 2000: The tephrochronology of Iceland and the North Atlantic region during the Middle and Late Quaternary: a review. *Journal of Quaternary Science* 15, 3–22.
- Hald, M. & Aspeli, R. 1997: Rapid climatic shifts of the northern Norwegian Sea during the last deglaciation and the Holocene. *Boreas* 26, 15–28.
- Hald, M., Dokken, T. & Hagen, S. 1996: Palaeoceanography of the European arctic margin during the last deglaciation. In Andrews, J. T., Austin, W. E. N., Bergsten, H. & Jennings, A. E. (eds.): *Late*

- Quaternary Palaeoceanography of the North Atlantic Margins*. 275–287. Geological Society Special Publication No. 111.
- Hald, M. & Hagen, S. 1998: Early Preboreal cooling in the Nordic seas region triggered by meltwater. *Geology* 26, 615–618.
- Hopkins, T. S. 1991: The GIN Sea - A synthesis of its physical oceanography and literature review 1972 to 1985. *Earth Science Reviews* 30, 175–318.
- Hu, F. S., Slawinski, D., Wright, H. E., Ito, E., Johnson, R. G., Kelts, K. R., McEwan, K. R. & Boedigheimer, A. 1999: Abrupt changes in North American climate during the early Holocene times. *Nature* 400, 437–440.
- IMAGES 101 1995: Les rapports de campagnes à la mer. IMAGES MD 101 à bord du *Marion-Dufresne* du 29 mai au 11 juillet 1995. Eds. Bassinot, F., Labeyrie, L. L'Institut Français pour la Recherche et la Technologie Polaires.
- Imbrie, J. & Kipp, N. G. 1971: A new micropaleontological method for quantitative paleoclimatology; Application to a late Pleistocene Caribbean core. In Turekian, K. K. (ed.): *The Late Cenozoic Glacial Ages*, 71–181. Yale University Press, New Haven.
- Jiang, H., Seidenkrantz, M.-S., Knudsen, K. L. & Eiríksson, J. 2001: Diatom surface sediment assemblages around Iceland and their relationships to oceanic environmental variables. *Marine Micropaleontology* 41, 73–96.
- Johannessen, O. M. 1986: Brief overview of the physical oceanography. In Hurdle, B. G. (ed.): *The Nordic Seas*, 103–127. Springer-Verlag, New York.
- Keigwin, L. D. & Jones, G. A. 1995: The marine record of deglaciation from the continental margin off Nova Scotia: *Paleoceanography* 10, 973–985.
- Klitgaard-Kristiansen, D., Sejrup, H. P., Hafliðason, H., Johnsen, S. & Spurk, M. 1998: A regional 8200 cal. yr BP cooling event in Northwest Europe, induced by final stages of the Laurentide ice-sheet deglaciation? *Journal of Quaternary Science* 13, 165–169.
- Koç Karpuz, N. 1989: *Surface sediment diatom distribution and Holocene palaeotemperature variations in the GIN Sea*. M.Sc. thesis, University of Bergen.
- Koç Karpuz, N. & Schrader, H. 1990: Surface sediment diatom distribution and Holocene paleotemperature variations in the Greenland, Iceland and Norwegian Seas. *Paleoceanography* 5, 557–580.
- Koç Karpuz, N. & Jansen, E. 1992: A high-resolution diatom record of the last deglaciation from the SE Norwegian Sea: Documentation of rapid climate changes. *Paleoceanography* 7, 499–520.
- Koç, N. & Jansen, E. 1994: Response of the high-latitude Northern Hemisphere to orbital climate forcing: Evidence from the Nordic Seas. *Geology* 22, 523–526.
- Koç, N., Jansen, E. & Hafliðason, H. 1993: Paleoceanographic reconstructions of the surface ocean conditions in the Greenland, Iceland and Norwegian Seas throughout the last 14 ka, based on diatoms. *Quaternary Science Reviews* 12, 115–140.
- Koç, N., Jansen, E., Hald, M. & Labeyrie, L. 1996: Late glacial-Holocene sea surface temperatures and gradients between the North Atlantic and the Norwegian Sea: implications for the Nordic heat pump. In Andrews, J. T., Austin, W. E. N., Bergsten, H. & Jennings, A. E. (eds.): *Late Quaternary Palaeoceanography of the North Atlantic Margins*, 177–185. Geological Society Special Publication No. 111.
- Lowe, J. J., Hoek, W. Z. and INTIMATE group 2001: Inter-regional correlation of palaeoclimatic records for the Last Glacial-Interglacial Transition: a protocol for improved precision recommended by the INTIMATE project group. *Quaternary Science Reviews* 20, 1175–1187.
- Lowe, J. J. & Turney, C. S. M. 1997: Vedde Ash layer discovered in a small lake basin on the Scottish mainland. *Journal of the Geological Society of London* 154, 605–612.
- Lozier, M. S., Brechner Owens, W. & Curry, R. G. 1995: The climatology of the North Atlantic. *Progress in Oceanography* 36, 1–44.
- Nesje, A. & Dahl, S. O. 1993: Lateglacial and Holocene glacier fluctuations and climate variations in western Norway: a review. *Quaternary Science Reviews* 12, 255–261.
- O'Brien, S. R., Mayewski, P. A., Meeker, L.-D., Meese, D.-A., Twickler, M. S. & Whitlow, S. I. 1995: Complexity of Holocene climate as reconstructed from a Greenland ice core. *Science* 270, 1962–1964.
- Renssen, H., Gorsse, H., Fichefet, T. & Campin, J.-L. 2001: The 8.2 kyr BP event simulated by a global atmosphere-sea-ice-ocean model. *Geophysical Research Letters* 28, 1567–1570.
- Sakshaug, E. & Skjoldal, H. R. 1989: Life at the ice edge. *Ambio* 18, 60–67.
- Sakshaug, E. & Slagstad, D. 1990: Light and productivity of phytoplankton in polar marine ecosystems: a physiological view. *Polar Research* 10, 69–85.
- Salvigsen, O., Forman, S. L. & Miller, G. H. 1992: Thermophilous molluscs on Svalbard during the Holocene and their palaeoclimatic implications. *Polar Research* 11, 1–10.
- Sancetta, C. 1999: Diatoms and marine paleoceanography. In Stoermer, E. F. & Smol, J. P. (eds.): *The Diatoms: Applications for the Environmental and Earth Sciences*, 374–386. Cambridge University Press, Cambridge.
- Sarnthein, M., Jansen, E., Arnold, M., Duplessy, J. C., Erlenkeuser, H., Flatøy, A., Veum, T., Vogelsang, E. & Weinelt, M. S. 1992: $\delta^{18}\text{O}$ time-slice reconstruction of meltwater anomalies at Termination I in the North Atlantic between 50° and 80°N. *NATO ASI Series* 12, 183–200.
- Sarnthein, M., Jansen, E., Weinelt, M., Arnold, M., Duplessy, J. C., Erlenkeuser, H., Flatøy, A., Johannessen, G., Johannessen, T., Jung, S., Koç, N., Labeyrie, L., Maslin, M., Pflaumann, U. & Schulz, H. 1995: Variations in the Atlantic surface ocean palaeoceanography, 50°–80°N: A time-slice record of the last 30000 years. *Paleoceanography* 10, 1063–1094.
- Schrader, H. J. & Gersonde, R. 1978: Diatoms and silicoflagellates. In Zachariasse, W. J., Reidel, W. R., Saflippo, A., Schmidt, R. R., Broelsma, M. J., Schrader, H. J., Gersonde, R., Drooger, M. M. & Broekman, J. A. (eds.): *Micropaleontological counting methods and techniques - an exercise on an eight metres section of the lower Pliocene of Capo Rossello, Sicily*, 129–176. Utrecht Micropaleontological Bulletins, The Netherlands.
- Schrader, H. J., Swanberg, I. L., Burckle, L. H. & Grølien, L. 1993: Diatoms in recent Atlantic (20°S to 70°N latitude) sediments: Abundance patterns and what they mean. *Hydrobiologia* 269/270, 129–135.
- Sejrup, H. P., Hafliðason, H., Flatebø, T., Klitgaard Kristensen, D., Grøsfjeld, K. & Larsen, E. 2001: Late-glacial to Holocene environmental changes and climate variability: evidence from Volda fjorden, western Norway. *Journal of Quaternary Science* 16, 181–198.
- Seppä, H. & Birks, H. J. B. 2000: July mean temperatures and annual precipitation trends during the Holocene in Fennoscandian tree-line area: pollen based climate reconstructions. *The Holocene* 11, 527–539.
- Stuiver, M., Pearson, G. W. & Braziunas, T. F. 1986: Radiocarbon age calibration of marine samples back to 9000 cal. yr BP. In Stuiver, M. & Kra, R. S. (eds.): *Proceedings of the 12th International ^{14}C Conference*. *Radiocarbon* 28, 980–1021.
- Stuiver, M., Reimer, P. J., Bard, E., Beck, J. W., Burr, G. S., Hughen, K. A., Kromer, B., McCormac, G., van der Plicht, J. & Spurk, M. 1998: INTCAL98 radiocarbon age calibration, 24000 – 0 BP. *Radiocarbon* 40, 1041–1083.
- Stuiver, M. & Reimer, P. J. 1993: Extended ^{14}C data base and revised CALIB 3.0 ^{14}C age calibration program. *Radiocarbon* 35, 215–230.
- Stötter, J., Wastl, M., Caseldine, C. & Häberle, T. 1999: Holocene palaeoclimatic reconstructions in northern Iceland: approaches and results. *Quaternary Science Reviews* 18, 457–474.
- Vorren, T. O., Vorren, K.-D., Alm, T., Gulliksen, S. & Løvlie, R. 1988: The last deglaciation (20000 to 11000 BP) on Andøya, northern Norway. *Boreas* 17, 41–77.
- Williams, K. M. 1986: Recent arctic marine diatom assemblages

from bottom sediments in Baffin Bay and Davis Straight. *Marine Micropaleontology* 10, 327–341.

Williams, K. M. 1993: Ice sheet and ocean interactions, margin of the East Greenland ice sheet (14 Ka to present): Diatom evidence. *Paleoceanography* 8, 69–83.

Appendix 1: Diatom nomenclature and taxonomic authorities

Actinocyclus curvatus Janish
Actinocyclus ehrenbergii Ralfs.
Asteromphalus robustus Castracane.
Bacterosira fragilis Gran.
Chaetoceros Ehr.
Coscinodiscus Ehr.
Fragilariopsis oceanica Hasle
Hemidiscus cuneiformis Wallich.
Nitzschia Hassall
Nitzschia bicapita Cleve.
Nitzschia capuluspala Grun.
Podosira Ehr.
Porosira glacialis (Grun.) E. Jørg.
Rhizosolenia alata Brightw.
Rhizosolenia bergonii Perag.
Rhizosolenia hebetata var. *hebetata* Sundström
Rhizosolenia hebetata var. *semispina* (Hensen) Gran.
Rhizosolenia styliformis Brightw.
Roperia tessellata (Roper) Grun.
Thalassionema nitzschioides (Grun.) Grun.
Thalassiosira angulata (Greg) Hasle
Thalassiosira leptopus (Grun.) Hasle & Fryxell
Thalassiosira decipiens (Grun.) E. Jørg.
Thalassiosira eccentrica (Ehr.) Cleve
Thalassiosira gravida Cleve
Thalassiosira lineata Jousé.
Thalassiosira nodulinea Hendey.
Thalassiosira nordenskiöldi Cleve.
Thalassiosira oestrupii (Ostenf.) Hasle
Thalassiosira pacifica Grans & Angst.
Thalassiosira trifulta Fryxell
Thalassiothrix longissima Cleve & Grun.

Appendix 2: The modern diatom-sea-surface temperature calibration data-set

This data-set consists of 139 core-top samples extending from 75°56.6'N to 42°01.8'N latitude and 49°45.0'W to 15°45.7'E longitude in the Nordic Seas and North Atlantic. All the samples were analysed by N. Koç and a total of 52 taxa was recorded.

To achieve taxonomic consistency between the diatom analyses of core MD95-2011 by C. J. A. Birks, some modifications had to be made to the taxonomy of the modern data-set. These were as follows:

- All the *Coscinodiscus* taxa were combined together as *Coscinodiscus* spp.
- All the *Nitzschia* taxa were combined together as *Nitzschia* spp., except for *N. bicapita* and *N. capuluspala*, which were kept separate.

All of the SST reconstructions presented here are based on this revised taxonomy of 37 taxa in the 139 surface sediments. The locations and the modern SST of these 139 samples are given in Birks (2001). The modern data-set has a range of August SST of 0–19.7°C (mean 8.6°C, median 8.8°C) and of February SST of –1–14.5°C (mean 4.2°C, median 4.3°C).

Summary statistics of the two transfer functions for August SST based on Imbrie and Kipp (I&K) factor analysis and weighted-averaging partial least squares (WA-PLS) regression are given as “apparent” statistics and as cross-validation estimates (Birks 1995) in Table A.2.1. Comparable statistics of the February SST transfer functions are given in Table A.2.2. Cross-validation based statistics for RMSE, r^2 , maximum bias, and % cumulative variances cannot currently be computed for the I&K method, so the apparent statistics for WA-PLS are given as well as the cross-validation statistics. Full details of the mathematical basis of these apparent and cross-validation statistics are given in ter Braak & Juggins (1993) and Birks (1995).

Listings of the I&K varimax factor score matrix, scaled varimax factor scores, and composition scores for the 37 taxa and the varimax factor components matrix and communalities for the 139 modern samples and of the WA-PLS loadings and beta coefficients (“optima”) for the 37 taxa and the scores for 139 modern samples for August and February SST are available on request to C. J. A. Birks.

Table A.2.1 Summary statistics for the transfer functions for August SST based on WA-PLS (1-6 component models) and Imbrie & Kipp (8 components). Transfer functions used in this study are given in bold.

| | Component | Apparent | | | | Cross-validation | | | |
|--------|-----------|-------------|-------------|-------------|-----------------|------------------|-------------|-------------|-----------------|
| | | RMSE | r^2 | Max. bias | % Cum. variance | RMSEP | r^2 | Max. bias | % Cum. variance |
| I&K | 1 | 1.34 | 0.80 | 2.12 | 13.6 | — | — | — | — |
| | 2 | 1.31 | 0.81 | 1.94 | 25.4 | — | — | — | — |
| | 3 | 1.30 | 0.83 | 1.28 | 43.9 | — | — | — | — |
| | 4 | 1.29 | 0.84 | 0.93 | 61.8 | — | — | — | — |
| | 5 | 1.26 | 0.84 | 0.91 | 70.0 | — | — | — | — |
| | 6 | 1.26 | 0.87 | 0.89 | 84.9 | — | — | — | — |
| | 7 | 1.25 | 0.88 | 0.88 | 92.7 | — | — | — | — |
| | 8 | 1.24 | 0.89 | 0.88 | 95.4 | — | — | — | — |
| WA-PLS | 1 | 1.14 | 0.91 | 3.2 | 90.8 | 1.20 | 0.90 | 3.80 | 89.9 |
| | 2 | 0.93 | 0.94 | 1.24 | 93.9 | 1.04 | 0.92 | 1.84 | 92.3 |
| | 3 | 0.86 | 0.95 | 0.79 | 94.8 | 1.01 | 0.93 | 1.78 | 92.8 |
| | 4 | 0.79 | 0.96 | 0.44 | 95.6 | 0.97 | 0.93 | 1.55 | 93.4 |
| | 5 | 0.76 | 0.96 | 0.54 | 95.9 | 0.93 | 0.94 | 1.40 | 93.9 |
| | 6 | 0.75 | 0.96 | 0.56 | 96.1 | 0.92 | 0.94 | 1.53 | 94.0 |

Max. = maximum; Cum. = cumulative; RMSE = root mean square error; RMSEP = root mean square error of prediction, r^2 = coefficient of determination.

Table A.2.2 Summary statistics for the transfer functions for February SST based on WA-PLS (1-6 component models) and Imbrie & Kipp (8 components). Transfer functions used in this study are given in bold.

| | Component | Apparent | | | | Cross-validation | | | |
|--------|-----------|-------------|----------------|-------------|-----------------|------------------|----------------|-------------|-----------------|
| | | RMSE | r ² | Max. bias | % Cum. variance | RMSEP | r ² | Max. bias | % Cum. variance |
| I&K | 1 | 1.84 | 0.72 | 3.04 | 13.6 | — | — | — | — |
| | 2 | 1.82 | 0.74 | 2.86 | 25.4 | — | — | — | — |
| | 3 | 1.79 | 0.78 | 2.04 | 43.9 | — | — | — | — |
| | 4 | 1.65 | 0.80 | 2.02 | 61.8 | — | — | — | — |
| | 5 | 1.51 | 0.81 | 1.98 | 70.0 | — | — | — | — |
| | 6 | 1.48 | 0.84 | 1.91 | 84.9 | — | — | — | — |
| | 7 | 1.42 | 0.86 | 1.54 | 92.7 | — | — | — | — |
| | 8 | 1.35 | 0.87 | 1.07 | 95.4 | — | — | — | — |
| WA-PLS | 1 | 1.34 | 0.87 | 2.37 | 87.0 | 1.39 | 0.86 | 2.87 | 86.1 |
| | 2 | 1.20 | 0.90 | 1.16 | 89.7 | 1.29 | 0.88 | 1.26 | 88.1 |
| | 3 | 1.08 | 0.92 | 0.92 | 91.6 | 1.23 | 0.89 | 1.07 | 89.1 |
| | 4 | 1.03 | 0.92 | 0.79 | 92.3 | 1.20 | 0.90 | 0.92 | 89.7 |
| | 5 | 0.99 | 0.93 | 0.82 | 92.9 | 1.18 | 0.90 | 0.97 | 90.0 |
| | 6 | 0.98 | 0.93 | 0.71 | 93.2 | 1.18 | 0.90 | 0.99 | 90.0 |

Max. = maximum; Cum. = cumulative; RMSE = root mean square error; RMSEP = root mean square error of prediction, r² = coefficient of determination.

Table A.3.1 - Listings of the Imbrie & Kipp Factors used in this study, their dominant species, and their inferred water-masses (Andersen 1998, Koç unpublished data).

| Factor | Water-mass | Dominant diatom taxa | % variance | % cumulative variance |
|----------|--|--|------------|-----------------------|
| Factor 1 | Arctic-Greenland Water | <i>Thalassiosira leptopus</i> , <i>Thalassiosira trifulta</i> | 13.6 | 13.6 |
| Factor 2 | North Atlantic Water | <i>Thalassiosira oestrupii</i> , <i>Thalassiosira nitzschioides</i> , <i>Nitzschia bicapita</i> , <i>Rhizosolenia bergonii</i> , <i>Roperia tessellata</i> | 11.9 | 25.4 |
| Factor 3 | Sub-arctic Water | <i>Rhizosolenia hebetata</i> v. <i>semispina</i> , <i>Rhizosolenia styliformis</i> , <i>Thalassiothrix longissima</i> , <i>Thalassiosira gravida</i> (vegetative) | 18.4 | 43.9 |
| Factor 4 | Norwegian-Atlantic Water | <i>Rhizosolenia styliformis</i> , <i>Rhizosolenia alata</i> , <i>Thalassiosira angulata</i> , <i>Thalassiosira nitzschioides</i> , <i>Thalassiosira gravida</i> (vegetative) | 17.9 | 61.8 |
| Factor 5 | Sea-ice | <i>Thalassiosira hyalina</i> , <i>Thalassiosira gravida</i> (spores), <i>Thalassiosira nordenskiöldii</i> , <i>Bacterosira fragilis</i> , <i>Fragilariopsis oceanica</i> | 8.2 | 70.0 |
| Factor 6 | Arctic Waters (Polar front) | <i>Thalassiosira gravida</i> (spores), <i>Thalassiosira gravida</i> (vegetative), <i>Actinocyclus curvatus</i> , <i>Rhizosolenia hebetata</i> var. <i>semispina</i> , <i>Rhizosolenia hebetata</i> var. <i>hebetata</i> | 14.9 | 84.9 |
| Factor 7 | Sub-arctic/ Norwegian Atlantic mixing Waters | <i>Thalassiosira gravida</i> (spores), <i>Rhizosolenia hebetata</i> var. <i>semispina</i> , <i>Thalassiosira nitzschioides</i> | 7.8 | 92.7 |
| Factor 8 | North Atlantic/ Sub-arctic mixing Waters | <i>Rhizosolenia styliformis</i> , <i>Thalassiosira gravida</i> (spores), <i>Rhizosolenia alata</i> , <i>Actinocyclus curvatus</i> , <i>Thalassiosira trifulta</i> , <i>Thalassiosira gravida</i> (spores), <i>Thalassiosira leptopus</i> | 2.7 | 95.4 |

Appendix 3: The eight varimax factors extracted from the modern diatom data-set

The eight Imbrie & Kipp varimax factors extracted from the 139 samples × 37 taxa modern data-set (Appendix 1), along with their dominant diatom taxa and inferred water-masses (Andersen 1998; Koç, unpublished data) are summarised in Table A3.1. Approximate equivalents with the six factors distinguished by Koç Karpuz & Schrader (1990) and Koç Karpuz & Jansen (1992) are given in Table A.3.2.

Factor 1 accounts for 13.6% of the total variance and has its highest sample loadings for samples underlying the Arctic waters of the Greenland Sea. The distribution of the factor closely parallels the distribution of Arctic Waters. Factor 2 (11.9%) has its highest loadings under the warm and saline North Atlantic Current Waters.

Table A.3.2 - Equivalent factors from this study and the six factors distinguished by Koç Karpuz & Schrader (1990) and Koç Karpuz & Jansen (1992) and the percent variance they account for.

| I&K Factor (This study) | Equivalent factor and % variance |
|-------------------------|----------------------------------|
| 1 | 2 p.p. (28.27%) |
| 2 | 5 (4.5%) |
| 3 | 2 p.p. (28.27%) |
| 4 | 1 (27.02%) |
| 5 | 3 (14.61%) |
| 6 | 2 p.p. (28.27%) |
| 7 | 4 (11.74%) + 6 (5.61%) |
| 8 | 4 (11.74%) + 6 (5.61%) |

Factor 3 (18.4%) is characteristic of the Sub-arctic waters of the west North Atlantic and the Arctic waters of the Iceland Sea. The distribution of Factor 4 (17.9%) parallels the poleward flow of the Norwegian – Atlantic Current. The spatial distribution of Factor 5 (8.2%) matches the limit of the sea-ice edge in winter. Factor 6 (14.9%) has a more complex distribution. In the Nordic Seas highest loadings occur under the East Icelandic Current and the Jan Mayen Polar Current whereas in the North Atlantic, high loadings occur as a belt following the Polar Front. Factor 7 (7.8%) has its highest loadings in waters between the Arctic Waters and the Norwegian-Atlantic Current Waters in the Nordic Seas and under the Subarctic Waters of the Labrador Sea. Factor 8, representing only 2.7% of the total variance, has its highest loadings in the area of transition and mixing between North Atlantic and Sub-arctic waters.

It is difficult to make detailed comparisons of these eight factors with the diatom assemblages recognised by Jiang *et al.* (2001) around Iceland because of differences in diatom taxonomy, geographical and environmental scales, and numerical methods used. Factors 4, 7, and 8 have similarities with Jiang *et al.*'s "warm-water diatom assemblage", factor 5 resembles the "sea-ice diatom assemblage" of Jiang *et al.* (2001), and factors 3 and 6 have affinities with the "cold-water diatom assemblage" of Jiang *et al.* There are no obvious similarities between the eight factors and the "mixing" and "coastal" diatom assemblages of Jiang *et al.* (2001), both of which occur in relatively shallow water depths near the shore, and in the case of the coastal assemblage, contain brackish and fresh-water diatoms as well as marine benthic and tychoplanktonic taxa.